Welding in the World (2025) 69:327–361
https://doi.org/10.1007/s40194-024-01847-w

REVIEW ARTICLE

Friction Stir-Based Techniques: An Overview

Noah E. El-Zathry[1,2] · Stephen Akinlabi[1] · Wai Lok Woo[1] · Vivek Patel[3] · Rasheedat M. Mahamood[1]

Received: 13 June 2024 / Accepted: 7 October 2024 / Published online: 17 October 2024

Abstract
Friction stir-based techniques (FSTs), originating from friction stir welding (FSW), represent a solid-state processing method catering to the demands of various industrial sectors for lightweight components with exceptional properties. These techniques have gained much more attraction by providing an opportunity to tailor the microstructure and enhance the performance and quality of produced welds and surfaces. While significant attention has historically been directed towards the FSW process, this review delves into the working principles of FSTs, exploring their influence on mechanical properties and microstructural characteristics of various materials. Additionally, emphasis is placed on elucidating the advancement of hybrid FSW processes for both similar and dissimilar metal components, aimed at enhancing welding quality through meticulous control of grain textures, structures, precipitation, and phase transformations. Finally, the review identifies current knowledge gaps and suggests future research directions. This review paper synthesises academic literature sourced from the Web of Science (WoS) and Scopus databases, supplemented by additional sources such as books from the last 15 years.

Keywords Friction Stir-Based Techniques · Friction Stir welding · Solid-State Processing · Additive manufacturing · And Hybrid FSW Processes

Nomenclature

AFSD	Additive Friction Stir Deposition
AM	Additive Manufacturing
AS	Advancing side
BM	Base material
FEM	Finite Element Method
FS	Friction Surfacing
FSAM	Friction Stir Additive Manufacturing
FSLW	Friction stir lap welding
FSP	Friction stir processing
FSSW	Friction Stir Spot Welding
FST	Friction Stir Techniques
FSW	Friction Stir Welding
GMAW	Gas Metal Arc Welding
GTAW	Gas Tungsten Arc Welding
HAZ	Heat Affected Zone
HSS	High-Speed Steel
HYB	Hybrid metal and extrusion bonding
IMCs	Intermetallic compounds
LSS	Lap Shear Strength
NZ	Nugget Zone
PAZ	Pin Affected Zone
PWHT	Post-weld heat treatment
RFSSW	Refill friction stir spot welding
RS	Retreating side
SAZ	Shoulder Affected Zone
SEM	Scanning Electron Microscope
SSFSW	Stationary shoulder FSW
SZ	Stir Zone
TEM	Transmission Electron Microscope
TMAZ	Thermomechanical Affected Zone
TWI	The Welding Institute
UTS	Ultimate Tensile Strength
XRD	X-ray Diffraction
YS	Yield Strength

Recommended for publication by Commission III - Resistance Welding, Solid State Welding, and Allied Joining Process.

✉ Noah E. El-Zathry
noah.elzathry@northumbria.ac.uk

[1] Department of Mechanical and Construction Engineering, Northumbria University, Newcastle upon Tyne, UK

[2] Mechanical Engineering Department, Benha University, Benha, Egypt

[3] Department of Engineering Science, University West, 46186 Trollhattan, Sweden

1 Introduction

Several industrial sectors, including transportation, aerospace, shipbuilding, and other key industries, are actively seeking ways to enhance the efficiency of machine components and parts. These requirements led to the development and revolution in the materials science and engineering field [1, 2]. To meet these demands, materials with exceptional characteristics, such as high-strength-to-weight ratios, including aluminium alloys, magnesium alloys, and titanium alloys, have been introduced for lightweight constructions and machine parts [3, 4]. However, the manufacturing and joining processes required to assemble large or complex structures using these alloys have encountered numerous challenges.

Traditionally, riveting has been a common joining technique, but it contributes to increased structural weight and can lead to fatigue crack initiation due to stress concentration. Fusion welding, while widely used, is susceptible to cracking and results in a large heat-affected zone (HAZ), significantly compromising the mechanical properties of assembled joints [5–7]. In response to these challenges, friction-based solid-state techniques have emerged as revolutionary solutions, redefining manufacturing, processing, and assembly practices in industries working with high-strength-to-weight materials [8–10]. These techniques have acquired remarkable success due to high efficiency, multi-material manufacturing ability, low energy consumption, low distortion, and typically high metallurgical properties [11, 12].

In this review paper, we compiled academic literature on Friction stir-based techniques (FSTs), primarily from the Web of Science (WoS) and Scopus databases, supplemented by additional sources such as books. Our data collection spanned the last 15 years, from 2009 to 2024. The aim is to offer a comprehensive overview of friction-based techniques, covering their principles, advantages, limitations, and the influence of various parameters on product quality across different materials. Additionally, the paper explores recent advancements in hybrid techniques that combine FSTs with other energy sources and welding methods. The review concludes by summarising key findings and proposing potential directions for future research in this evolving field.

2 Friction stir-based techniques

Friction stir-based techniques (FSTs) have demonstrated superior performance across various industrial sectors, serving as a viable alternative to traditional fusion-based methods [13]. FSTs operate by generating frictional heat that remains below the material's melting point but near its recrystallization temperature. The controlled heat promotes interatomic diffusion and material intermixing, resulting in the creation of robust bonds between the joining or depositing materials. Based on their operating principles, we can broadly classify these techniques into two categories. Welding techniques used to join two or more plates fall under the first category. Processing methods used to enhance the properties of materials fall under the second category. Figure 1 depicts this classification. It is worth mentioning that tools used in FSTs can either be consumable or non-consumable, depending on the specific application. Techniques such as Friction Stir Additive Manufacturing (FSAM) and Friction Stir Welding (FSW) typically use non-consumable tools. On the other hand, processes such as Additive Friction Stir Deposition and Friction Surfacing utilize consumable tools that gradually deplete during the operation. This classification is depicted in Fig. 1, based on references [14–17]**.** It is worth mentioning that tools used in FSTs can either be consumable or non-consumable, depending on the specific application. Techniques such as Friction Stir Additive Manufacturing (FSAM) and Friction Stir Welding (FSW) typically use non-consumable tools. In contrast, other processes like Additive Friction Stir Deposition and Friction Surfacing employ consumable tools, which are gradually consumed during the operation [18]. This section aims to comprehensively cover these FSTs, detailing their principles, applications, as well as their respective advantages and limitations.

2.1 Friction Stir welding (FSW)

In 1991, a solid-state welding technique called FSW was developed at The Welding Institute (TWI) in the UK [19]. This technique proved its efficiency in joining different types of materials that face difficulties during joining with traditional techniques. Additionally, the FSW process has proven its efficiency in welding several materials, including aluminium (Al) alloys [20–23], copper (Cu) alloys [24–27], titanium (Ti) alloys [28–31], magnesium (Mg) alloys [32–35], steel alloys [36–40], and dissimilar alloys, including Al/Cu alloys [41], Al/Mg [42] Al/Ti [43], Ni/Ti [44], and Mg/Ti [4], among others. FSW of dissimilar alloys with close melting temperatures is most effective, as optimising welding parameters can eliminate the formation of thick, continuous interlayers of intermetallic compounds [45]. However, some defects associated with intermetallic compounds and their heterogeneous distribution in dissimilar joints, such as reduced mechanical properties and thermal and electrical conductivity, may arise [29]. These defects can be mitigated through

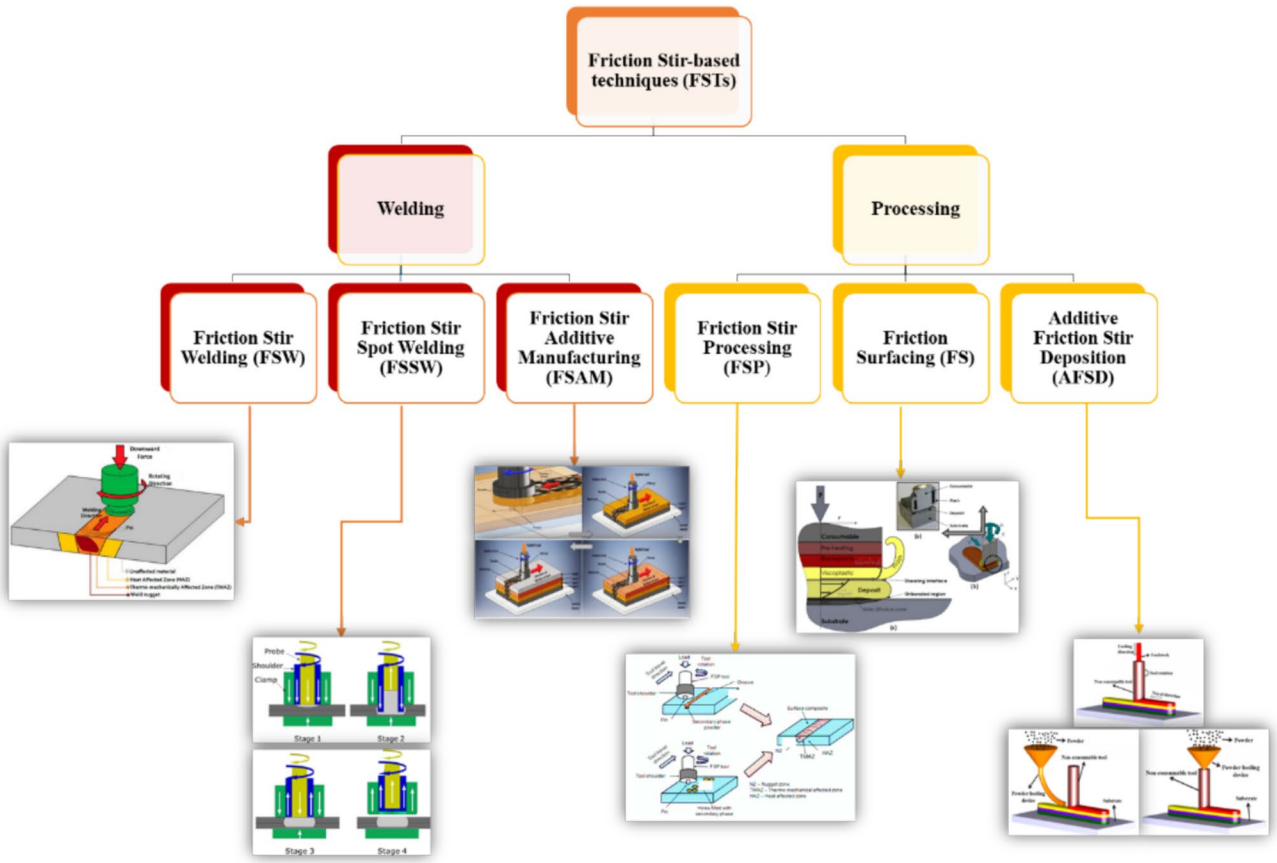

Fig. 1 Friction Stir-Based Techniques (FSTs) classification

various methods, including optimising welding parameters [46–48], utilising cooling techniques to minimise heat dissipation [49, 50], incorporating additive materials [51–54], or employing hybrid-FSW approaches [55, 56].

The FSW process has several parameters, such as tool material, rotational speed, traverse speed, tilt angle, tool position, and tool geometry, that significantly affect welded joints' metallurgical and mechanical properties [57]. Figure 2- a) displays a schematic diagram of the FSW process and welding zones.

FSW is a foundational technique among FSTs and shares many principles and processes with other FST methods, making it an ideal starting point for detailed discussion. In this section, we will delve into the principles and parameters of the FSW process, examining their influence on the thermal cycle, material flow, and overall joint quality. This exploration will provide a comprehensive understanding of how these factors interact and affect the performance of the weld, offering insights that are broadly applicable across various FST methods.

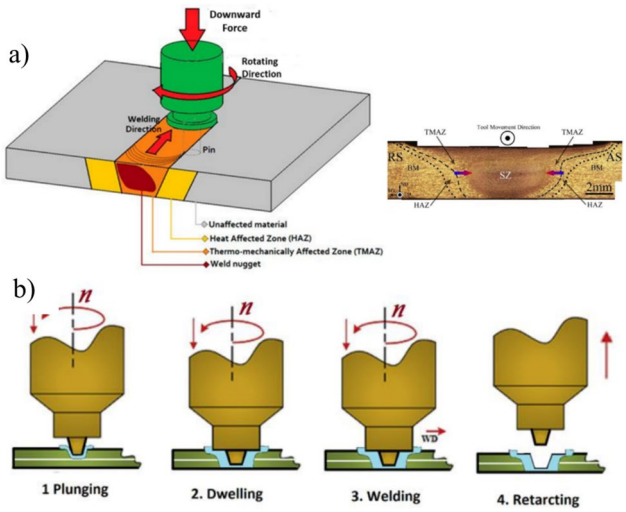

Fig. 2 **a** FSW process schematic and welding zones [14] and (**b**) FSW process steps [58]

2.1.1 FSW process principles

The principle of the FSW process involves utilizing a specially designed rotating tool with a shoulder and pin, and it is carried out through four distinct steps. The plunging step initiates the process, pressing the tool vertically downward with axial force, enabling the rotating pin to penetrate the joint between the two pieces of material for welding. The dwelling step initiates when the tool shoulder touches the workpiece surface. During this phase, the friction between the rotating tool and the workpieces generates heat, softening the material. Once the temperature exceeds the recrystallization point of the material but remains below its melting point, the welding step begins. At this stage, the tool traverses the joint line, maintaining axial force. The shoulder continues to generate heat through friction and deformation, while the pin stirs and mixes the softened material, creating a solid-state weld. Finally, after completing the weld, the tool retracts from the workpiece, leaving an exit hole at the end of the weld line [59].

2.1.2 FSW process parameters

FSW process parameters are shown in Fig. 3. The quality of friction stir welded (FSWed) joints is intricately linked to various parameters, making their optimisation crucial for achieving optimal performance. Among these parameters, tool speeds (both rotational and traverse) play a pivotal role in the FSW process. They directly affect the thermal cycle and the amount of heat generated for material plasticization. Observations have revealed that decreasing traverse speed and increasing rotational speed result in grain growth and material softening [60–63]. Tool geometry, encompassing both shoulder and pin design, plays a crucial role in regulating heat generation and material flow during the welding process. However, its impact on joint quality is relatively less pronounced compared to tool speeds [64–66]. Additionally, factors such as plunge depth, representing the extent of tool penetration into the workpiece, and tilt angle, indicating the angle between the spindle's axis and the workpiece, significantly influence welded joint quality. These parameters affect material mixing, weld depth, and the shape of the weld zone [67–69].

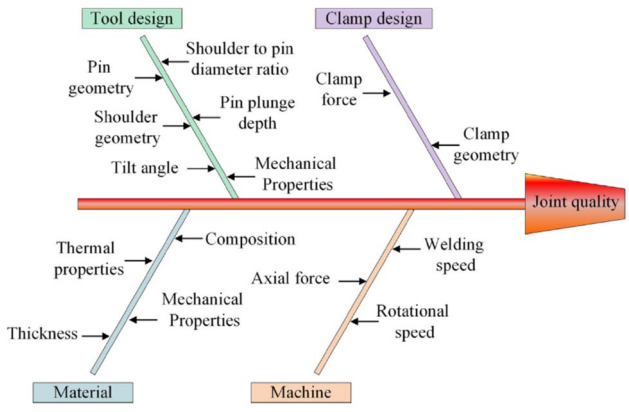

Fig. 1. FSW parameters and conditions.

Fig. 3 FSW Parameters [70]

2.1.3 FSW joint microstructure

In the welding process, four distinct zones are formed: the stir zone (SZ), thermos-mechanically affected zone (TMAZ), heat affected zone (HAZ), and base material (BM) zone, as illustrated in Fig. 2. The SZ, situated at the center of the weld, experiences the highest levels of heat and deformation, resulting in a complex grain structure with prominent onion ring features. These features arise from the successive shearing and deposition of plasticized material around the tool. Additionally, the SZ can be further subdivided into the Shoulder Affected Zone (SAZ) and the Pin Affected Zone (PAZ), which varies based on the tool geometry [71]. The TMAZ, undergoes plastic deformation and microstructural changes, leading to elongated, narrower, and relatively coarser grains compared to those in the SZ. This is attributed to dynamic recovery, where temperatures and strains are inadequate for recrystallization. In contrast, less deformation is always observed in the HAZ, which is accompanied by grain coarsening due to the input heat effect [72].

The mechanical properties of FSWed joints are significantly influenced by the joint microstructure, which can be enhanced by controlling the previously mentioned process parameters. The following section will summarise research papers that investigate the effects of various FSW process parameters on joint quality.

2.1.4 Previous studies on the FSW process

Several studies were carried out on the FSW process in an attempt to understand the process concepts and parameters' effects on the welded joints. In addition to butt welding joints, the FSW process has demonstrated high performance in lap welding, as evidenced by studies [73–77], and T-joint welding, as demonstrated by research [67, 78–80]. Various modifications have been implemented in the FSW process to improve its quality. These include the utilisation of specially designed tools [18], filler material [81], and hybrid FSW techniques [82], which will be discussed in detail in Sect. 3. Additionally, inherent challenges in FSW, such as keyhole defects, back support issues, and weld thinning, along with recent advancements to address these problems, are discussed in [83]. The studies focusing on FSW applied to metal matrix composites are covered in [84]. This section aims to explore key aspects, including the optimisation of

FSW process parameters for similar and dissimilar materials, the thermal behaviour and material flow during FSW, the role of heat treatment, and their combined effects on microstructural evolution and mechanical properties. The key findings from these studies are summarised below:

As previously mentioned, optimising FSW process parameters significantly affects the amount of heat input and, in turn, enhances the quality of welded joints. Ahmed et al. [85] conducted an optimisation study using traverse and rotational speeds as input parameters to examine their impact on the joint quality of dissimilar aluminium alloys AA5083/AA5754 and AA5083/AA7020. The study revealed that high heat input resulted in tunnel defects, as shown in Fig. 4. However, at optimal parameters, the welded joint efficiency reached up to 97% and 98%. In the AA5083/AA5754 joint, the hardness profile was observed to be low at the SZ due to the loss of cold deformation strengthening. Conversely, a high hardness value was noted in the SZ of the AA5083/AA7020 joint, attributed to the latter's high-strength alloy nature. Placing AA7020 at the advancing side led to higher joint strength and efficiency. Figure 5 shows the fracture surface of AA7020/AA5083 joint tensile test samples.

The impact of FSW tool speeds on the tensile properties of AA 2024-T3 welded lap joints was investigated by Viscusi et al. [86]. Using a central composite design and the steepest ascent algorithm, they optimised process parameters, identifying 1250 rpm and 4 mm/s as the optimal welding speeds. Similarly, Wang et al. [87] applied this welding technique to AA 2024-T6 aluminium alloy, focusing on tensile properties and defect formation across various welding speed ratios. Their findings underscored the importance of the viscous-to-rheological layer thickness ratio in weld quality. Defect-free joints were achieved when the viscous layer was thicker, while void defects occurred when the ratio of rotational to traverse speed decreased. Zamani et al. [88] employed the FSW process to weld Al-SiC 20% composite plates, with optimisation of tool rotational and traverse speeds using response surface methodology (RSM). They investigated various

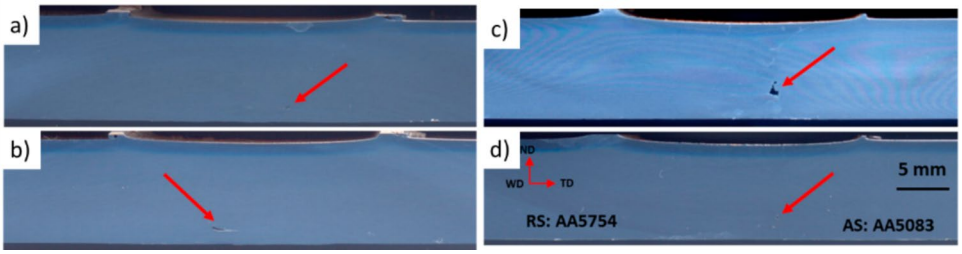

Fig. 4 Cross-sections of FSWed joints AA5083/AA5754. Arrows refer to the tunnel defects: **a** 400 rpm, 20 mm/min, (**b**) 600 rpm, 20 mm/min, (**c**) 600 rpm, 40 mm/min and (**d**) 600 rpm, 60 mm/min [85]

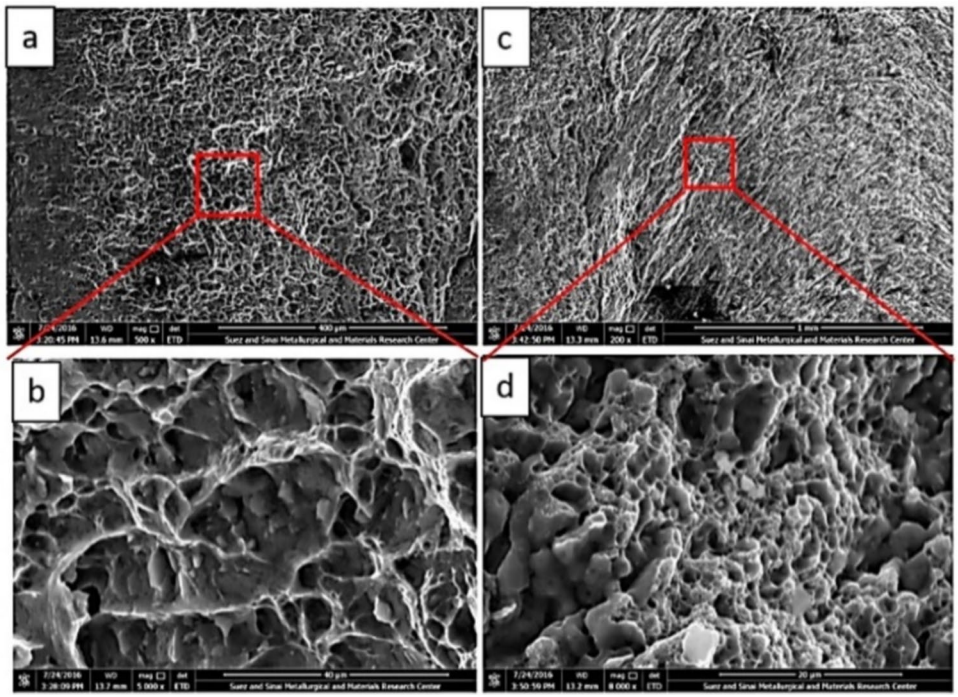

Fig. 5 Shows the fracture surface of AA7020/AA5083 joint tensile test samples [85]

mechanical properties of the welded joint, including tensile strength, hardness, and residual stresses. The study revealed that tool speeds significantly influenced the quality of the welded joint. The lowest mechanical properties were observed at high rotational speed and low traverse speed (1200 rpm and 40 mm/min, respectively). Conversely, optimal parameters were identified at 1400 rpm rotational speed and an increased traverse speed of 70 mm/min.

Another critical parameter is the tool pin geometry, which significantly influences both the frictional heat generated and the material flow during the process. The frictional heat primarily originates from the friction between the shoulder and the welded plates, which softens the material beneath the shoulder. Meanwhile, the specific shape of the pin plays a vital role in stirring and mixing this softened material, directly impacting the weld's quality and integrity. The combined effect of shoulder friction and pin geometry ensures proper material flow, which is essential for achieving a defect-free and mechanically robust weld. The effect of different pin shapes was explored in a study by Sun et al. [89] to understand its effect on the mechanical properties and material flow in FSW of dissimilar joints of AA 2024-T6 and AA 6061-T6. They tested three different pin shapes: conical thread, conical cam thread, and deep groove thread. The researchers found that thread geometry significantly influenced material flow and downward movement during the welding process. The material in the SZ primarily originated from the advancing side. Among the tested pin shapes, the conical cam thread pin produced the highest-quality joint, characterised by a minimal grain size ranging from 7 to 12 µm in the SZ. Conversely, the conical thread pin resulted in the lowest tensile strength of the welded joint. Further investigation on the effects of tool geometry can be found in [57, 90, 91].

Other studies extended the analysis to additional parameters such as tool tilt angle, shoulder pinching gap, tool pin position and shape. Wang et al. [92] and Khan et al. [93] studied the impact of tool tilt angle, while Rabiezadeh et al. [94] highlighted the significance of the shoulder pinching gap in achieving high joint efficiency by reducing grain size in the SZ. Sahali et al. [95] focused on the impact of different tool pin shapes—straight cylindrical, taper, and threaded cylindrical—on power consumption and tensile strength in AA3004-H32 joints. Their results indicated that power consumption is directly related to rotational speed, with the straight cylindrical pin consuming the least power. Tensile strength was mainly affected by rotational speed and pin profile, with traverse speed also influencing welding costs. These results are in good agreement with Janeczek et al. [96]. Ahmed et al. [97] investigated the effects of tool pin eccentricity and traverse speed on the mechanical properties and grain structure of FSWed AA5754-H24 aluminium alloy. They found that an increase in traverse speed led to a reduction in SZ grain size and an improvement in ultimate tensile strength and yield strength.

The thermal behaviour and material flow during the FSW process play a critical role in determining the weld microstructure, which directly impacts the mechanical properties of the joint. For instance, in welded aluminium alloys, factors such as grain size and precipitate distribution significantly influence joint strength. By understanding and controlling the thermal behaviour and material flow during welding, it is possible to optimise these microstructural features and, consequently, enhance the mechanical properties of the weld. Recognising this, numerous studies have been conducted to explore material flow behaviour and thermal cycle during FSW under various conditions, aiming to identify the optimal parameters for achieving superior joint performance. The studies focus on the simulation of material flow in the FSW process using numerical modelling approaches are summarised in [98, 99]

The thermal behaviour of the FSW process was investigated by Salih et al. [100], who examined the impact of FSW tool speeds (rotational and traverse) on the material flow behaviour and thermal cycle of AA6082-T6 welded joints. They found that these parameters significantly influenced welded joint quality, microstructure characteristics, and defect formation. At 1800 rpm and 20 mm/min, the temperature increased to 593 °C (0.9 of the melting temperature), demonstrating their substantial effect on thermal behaviour. Increasing traverse speed improved welded joint strength by re-precipitating strengthening precipitates and refining grain size, leading to higher fatigue life. In a related study, Liu et al. [101] developed a fully coupled thermo-mechanical model for AA6082-T6 aluminium alloy to analyse temperature distribution and material deformation during FSW. They considered tool rotational direction and plate geometry variations. The authors concluded that welded plate geometry influenced temperature distribution, while tool rotational direction affected heat distribution and strain distribution. Higher strain was observed on the advancing side compared to the retreating side. For further understanding of the material flow during FST, numerical simulations were conducted in the study by Kalinenko et al. [102] to explore the relationship between SZ microstructure characteristics and temperature conditions during FSW of AA6061 aluminium alloy. Their findings revealed that, under low heat input conditions, a large grain size (~ 100 µm) emerged in the SZ as a result of the competition between normal and abnormal grain growth. Conversely, under high heat input conditions, microstructural stability was observed in the SZ due to a combination of a high fraction of particles and relatively coarse grains. The researchers concluded that abnormal grain growth occurred rapidly during the early stages of post-weld solution treatment, a phenomenon elucidated

by Humphrey's cellular growth model. These findings highlight the significant influence of heat treatment on the quality of welded joints, prompting further investigations into its effects.

The thermal behaviour of the FSW process is significantly influenced by heat treatment, which affects heat distribution, the material's response to generated heat, and the evolution of the weld microstructure. Heat treatments are typically classified into pre-weld and post-weld treatments, each playing a crucial role in shaping the final properties of the weld. Therefore, a deep understanding of heat treatment parameters is essential for optimising and achieving the desired weld characteristics in FSW. Khalilabad et al. [103] explored friction stir welded dissimilar joints between AA2198 and AA2024. They noted that post-weld heat treatment (PWHT) strengthened the HAZ of AA2198 without abnormal grain growth in AA2024. However, challenges arose due to the alloys' differing heat-treatment responses and uneven work hardening. Wang et al. [104] examined heat treatment's impact on FSWed AA7050-T76 joints, comparing as-welded plates with those undergoing solid-solution treatment before welding and subsequent T76 aging. The optimised sequence reduced copper segregation and minimised precipitate coarsening, improving corrosion resistance and achieving consistent microchemistry across FSW zones. Similarly, Gupta et al. [105] found that PWHT at 121 °C for 24 h enhanced the corrosion resistance and mechanical properties of FSW AA 7017-T651 joints, especially at higher welding speeds. Dong et al. [106] reported that combining PWHT with water-cooling significantly improved welded joint quality, with direct artificial aging preserving equiaxed grains and solution heat treatment followed by aging showing abnormal grain growth (AGG). Overall, these studies collectively illustrate the crucial role of heat treatment in optimising the mechanical and corrosion properties of FSWed aluminium alloys, highlighting the importance of tailored heat treatment processes for different alloy compositions and welding conditions.

As an attempt to reduce the heat transferred from the FSW tool to the spindle, Li et al. [107] investigated methods to isolate heat flow from the FSW tool to the spindle through experimental and numerical models. They tested ten FSW tools with three different insulation features: reducing cross-sectional area, varying contact area between the tool holder and shank, and applying a thermal coating to the tool shank. Results showed that the tool combining all three insulation features achieved high heat insulation efficiency, reducing heat transferred to the spindle by 52% compared to conventional tools. However, they found that coating with a 0.3 mm layer of Y2O3-stabilized ZrO2 was less effective than reducing the tool's cross-sectional area. However, [100, 101, 107] have primarily focused on the impact of tool speeds on joint quality, overlooking the significance of exploring interactions among additional parameters such as plunge depth, dwell time, and tool geometry. This oversight impedes the development of a comprehensive understanding of friction stir welding processes. Consequently, there is a critical need to delve deeper into the interplay of various factors to advance the optimisation of welding procedures, thereby enhancing joint quality and performance. Although Li et al. [107] investigated heat isolation methods from the FSW tool to the spindle, their study mainly examined insulation features. More research is needed to evaluate the long-term durability and practicality of these methods in real-world FSW applications.

2.1.5 Hybrid metal and extrusion bonding (HYB)

However, the FSW process has some limitations when using filler material. In the last decade, these limitations were solved by the hybrid metal and extrusion bonding (HYB) invention [81]. HYB is a novel solid-state welding technique that combines the advantages of Gas Metal Arc Welding (GMAW) and FSW, using a filler material through solid-state welding with an adequate groove or joint design [108]. The microstructural and mechanical properties of the welded

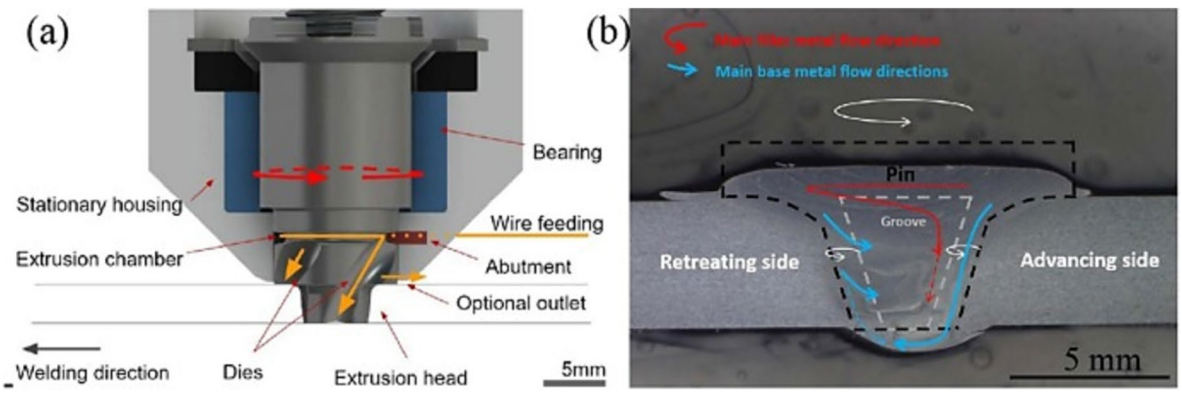

Fig. 6 HYB process (**a**) schematic (**b**) macrostructure [110]

joint of aluminium alloy can be enhanced by the injection of an aluminium FM continuously into the weld groove [109]. Sandnes et al. [110] conducted an investigation on the effect of the HYB process utilising AA6082-T6 aluminium alloy plates with a thickness of 4 mm and AA6082-T4 filler material with a wire diameter of 1.2 mm. The plates were configured in an I-groove shape with a separation of 3 mm and a pin diameter greater than 3 mm to ensure complete contact between the pin and the groove. Figure 6 (a) shows the HYB process. The welding parameters included a rotational speed of 400 rpm, a traverse speed of 6 mm/s, and a wire feed rate of 142 mm/s. Results indicated the production of sound joints within a temperature range of 350 °C to 400 °C, below the reported peak temperature for FSW. The authors suggested this temperature range to mitigate joint softening and enhance joint quality. Additionally, the formation of metallic bonding via oxide dispersion along the groove side walls was observed, as shown in Fig. 6 (b). Comparative analysis with GMAW and FSW revealed that the mechanical properties of HYB joints surpassed those of GMAW but fell short of FSW joints. Similar materials [109, 111], dissimilar materials [112–114] and various joint configurations, such as butt, T, and lap joints, can be performed by HYB [115]. While the HYB process shows promise in enhancing the microstructural and mechanical properties of welded joints, there is a lack of comprehensive studies evaluating its effectiveness across different materials, joint configurations, and welding conditions. Further research is needed to assess its performance under various parameters and scenarios to determine its broader applicability and potential limitations.

In summary, the FSW process offers numerous advantages over traditional fusion techniques, including higher welding joint efficiency, compatibility with a wide range of materials, reduced power consumption, the absence of toxic gases, and an eco-friendly approach. However, it also presents certain limitations, such as the need for specialised equipment, requirements for high downward force, exit hole defects and reduced flexibility compared to conventional welding processes.

2.2 Friction Stir spot welding (FSSW)

Mazda Corporation, Japan, developed Friction Stir Spot Welding (FSSW) as a solid-state welding technique in 1993 [116]. Unlike FSW, FSSW does not involve traverse movement; instead, joining occurs under high downward force and rotational action of the tool, as depicted in Fig. 7. Upon exiting, the tool leaves behind a keyhole. After the exiting step of the tool, a keyhole leaves behind the pin [8]. To address this issue, Refill Friction Stir Spot Welding (RFSSW) was introduced at Helmholtz-Zentrum Geesthacht in Germany in 1999 [8]. RFSSW utilises a probless tool, as illustrated in Fig. 8. During RFSSW, as demonstrated in step 2, the plasticized material elevates the pin as the shoulder descends. Following the spot joint, as depicted in step 3, the sleeve retracts and the pin plunges. Subsequently, the tool retracts after completing the weld formation. The welding process employs a clamping ring to securely hold the workpieces and prevent the plasticized material from flashing outside the welding zone [117].

Chu et al. [118] delved into the impact of FSSW probless shoulder features on the joint efficiency of AA2198-T8, incorporating both experimental and numerical simulation methods. The study explored three shoulder features: flat,

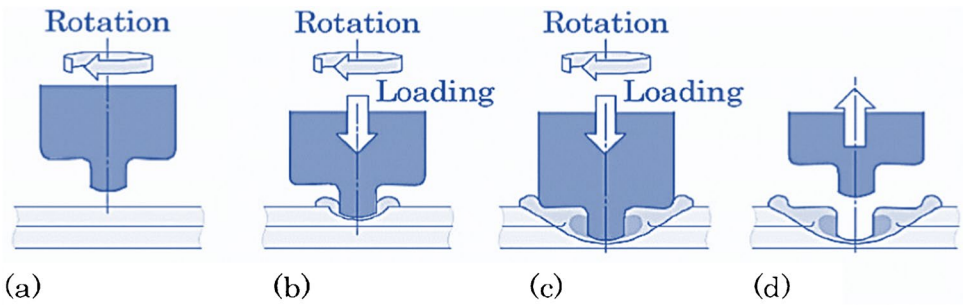

Fig. 7 FSSW process steps: **a** rotating, (**b**) plunging, (**c**) dwelling, (**d**) exiting [8]

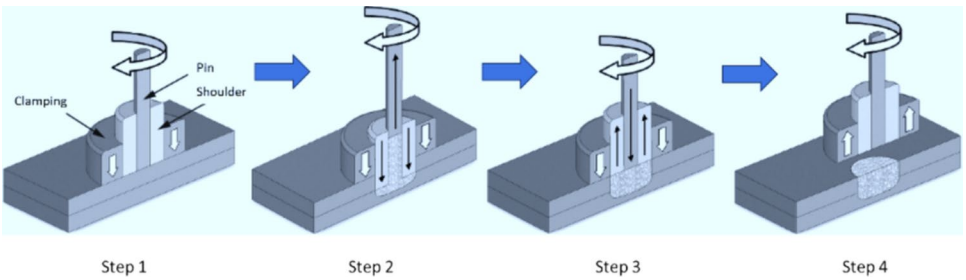

Fig. 8 RFSSW process [8]

annular, and involute. Upon evaluation, it was observed that the involute tool produced sound joints. Additionally, they noted that at higher rotational speeds, the dwell time should be reduced to prevent excessive material squeezing and the formation of flash defects. Yan et al. [119] conducted a study to perform FSSW joints between Polyamide 6 (PA6) and Acrylonitrile Butadiene Styrene (ABS) using a tooth-shaped pin tool. Various rotational speeds were explored, ranging from 250 to 500 rpm. Defects were observed at rotational speeds of 250 rpm and 500 rpm due to the presence of large PA6 particles. Conversely, smaller particles of PA6 (measured in microns or nanometers) were observed at 350 rpm. The Taguchi method (L9) was employed to optimise welding parameters. The rotational speed range chosen for this study was limited, considering that the maximum lap shear fracture load of 2034 N was achieved under the optimal parameters: 1000 rpm rotational speed, 40 s dwell time, and 11.5 mm plunge depth. The previous two papers did not explore the impact of the cooling process during FSSW. However, Wang et al. [120] applied the FSSW technique to weld 1.2 mm thick DP1180 steel with and without water cooling. The process parameters included rotational speeds of 400 and 600 rpm, a 10-s dwell time, a 1 mm plunge depth, and a 5 mm/min plunge speed. Water cooling was found to improve joint quality, eliminating hook defects and achieving a maximum lap shear strength of 17.9 kN. Figure 9 shows the macrostructure and fractured samples at 600 rpm. These improvements were attributed to grain refinement and effective tool softening restraint underwater. As the development of the FSSW process continues, Fu et al. [121] introduced a novel tool for RFSSW, enabling the utilisation of varying rotational speed values and directions for both the pin and shoulder. This innovation was applied to AM50 Mg alloy, with results compared to those obtained through traditional RFSSW methods. The study revealed a lap shear strength increase of 50% compared to traditional RFSSW. Additionally, this technique demonstrated efficacy in welding other alloys, including similar aluminium alloys and Mg/steel dissimilar joints.

In summary, FSSW stands as a notable technique for welding thin materials, offering advantages such as minimal material distortion, low residual stress, and a refined weld structure. However, FSSW does come with limitations, including the occurrence of exit holes and its applicability to thin sheets only. Additionally, it exhibits less flexibility compared to traditional welding techniques, requiring a rigid fixture for operation. Nonetheless, challenges such as exit hole formation can be mitigated through innovations like probless-FSSW or Refill Friction Stir Spot Welding (RFSSW). Studies addressing the challenges of FSW and FSSW in dissimilar Al-alloys, such as inhomogeneous structure formation in the SZ, low material plasticity, and inhomogeneous mixing due to the insufficient heat input, are summarised in [122] and [123].

2.3 Friction Stir additive manufacturing (FSAM)

Friction Stir Additive Manufacturing (FSAM) is an innovative method that merges FSTs with the principles of additive manufacturing (AM) [124]. This technique can be classified into two main categories based on the underlying process. The first category involves the combination of FSW with AM, while the second category integrates AM with friction deposition [18]. This section will concentrate on the first category, while Sect. 2.6 will delve into the second category after discussing friction surfacing techniques.

The process of FSAM is similar to the FSW of lap joints, involving the layer-by-layer joining of multiple flat plates and thorough cleaning between each plate. However, FSAM incorporates additional parameters like reheating and re-stirring into the process. A non-consumable rotating tool with a pin plunges into the overlapping plates and then traverses in a specific direction, as depicted in Fig. 10 [125]. Similar to other FSTs, the frictional heat generated between the tool and plates aids in softening and mixing the materials beneath the tool [9].

The FSAM process offers several advantages over fusion-based additive manufacturing (AM) methods. It consumes significantly less energy, using only about 2.5% of the energy required by fusion-based AM processes. Additionally, FSAM produces structurally efficient and effective

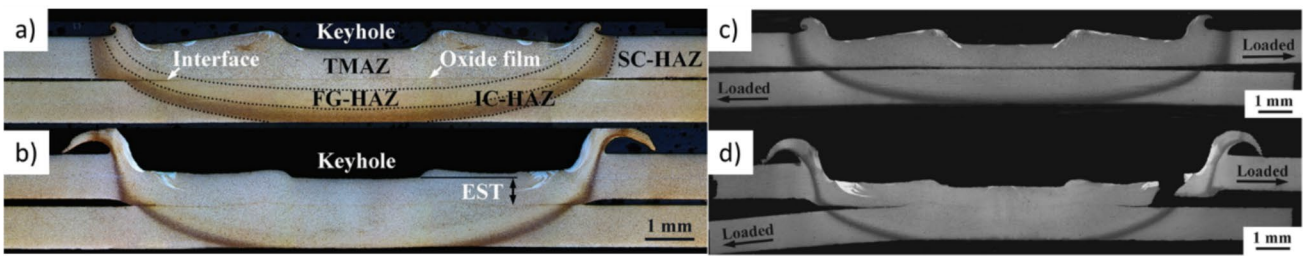

Fig. 9 Macrostructure of the typical joints at 600 rpm (**a**) without water cooling, (**b**) with water cooling and fractured samples of typical joints at 600 rpm: (**c**) without water cooling and (**d**) with water cooling [120]

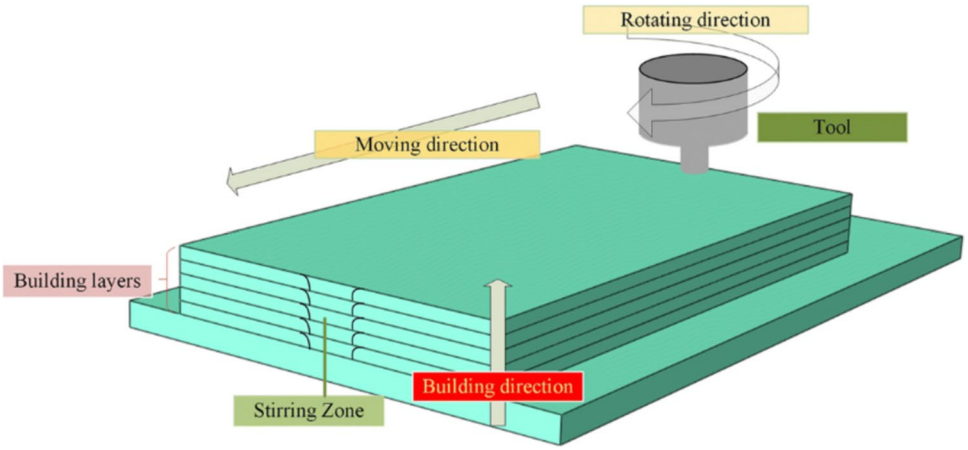

Fig. 10 FSAM process [125]

parts, with optimal consolidation, leading to high-quality components with enhanced mechanical properties [9, 126].

The hardness properties and fracture behaviour of joints between cast AA2050 and wrought AA2050-T3 were investigated by Lu and Reynolds [127]. Each plate measures 12 mm in thickness. Prior to processing, the surfaces of the plates were thoroughly cleaned of contaminants using a grinding disc and alcohol wipe. A tool configuration with a 28.6 mm shoulder diameter and a threaded-tapered pin length of 12.85 mm was employed. The process involved two passes with a 4 mm offset between the centres of the two lines. The study revealed an inhomogeneous distribution of hardness and properties distinct from those of the parent alloys, as shown in Fig. 11. Crack propagation during fracture tests was found to correlate with the traverse direction. Zhang et al. [128] conducted an experimental and numerical study on the FSAM process using a 4 mm thick AA6061-T6 plate and an 8 mm thick AA-6082 substrate plate. Their findings indicated that increasing the number of plates led to a decrease in the peak temperature of the newly added layer. Additionally, they observed that re-stirring and re-heating at lower temperatures enhanced the tensile properties and promoted the distribution of fine grains. Interestingly, they noted that there was no significant improvement in the mechanical properties after adding 2–3 layers. These results are consistent with results in [129]. However, the number of layers is related to the layer thickness. Hence, new efforts should be made to improve the performance of FSAM by optimising process parameters, including layer thickness, tool configuration, and traverse speed, to attain superior mechanical properties. Additional research and summary of FSAM type of machine for fabrication, materials mechanical properties such as grain refinement, and microhardness evaluation can also be explored in [18, 126, 130]

In summary, FSAM offers numerous advantages, including the ability to improve the properties of wrought

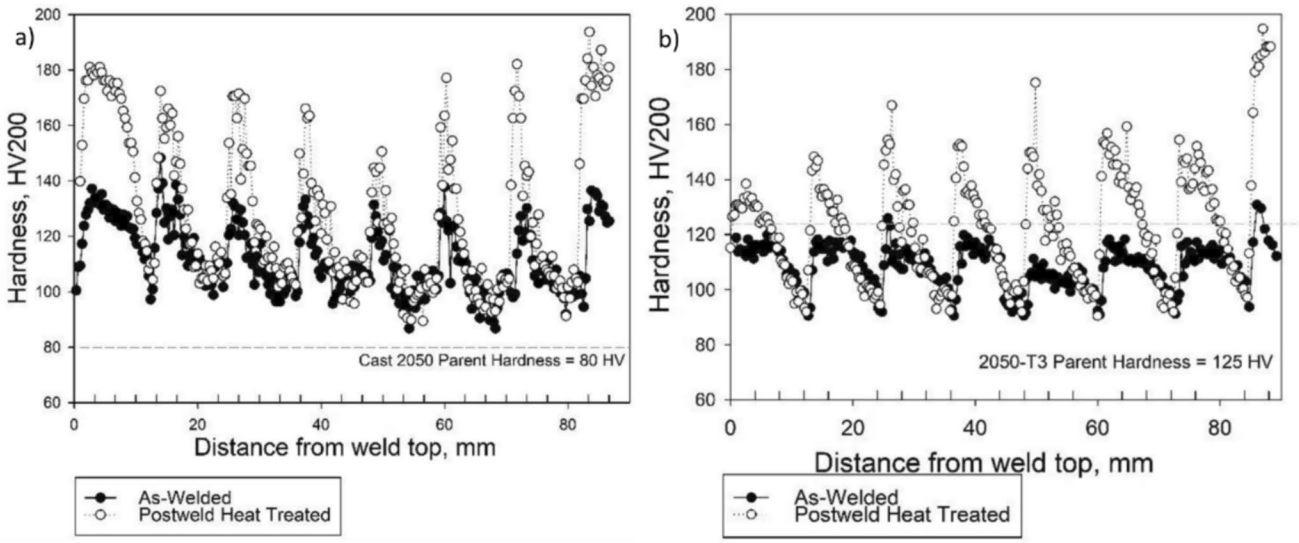

Fig. 11 Hardness distribution through (**a**) cast 2050 aluminium alloy build and (**b**) weld depth for AA2050-T3 build [127]

structures and fabricate intricate shapes without material waste or extensive machining. However, challenges include higher tool wear rates and the potential for an inhomogeneous microstructure.

2.4 Friction Stir processing (FSP)

Friction Stir Processing (FSP), a solid-state technique, emerged as a potential derivative from FSW in 1991 at TWI, UK [13]. Depending on the desired material properties and application, one can conduct FSP with or without the incorporation of reinforcement particles. The introduction of reinforcement particles can significantly enhance the mechanical properties of the processed material. FSP has been applied for various purposes, such as enhancing the microstructure and mechanical properties of materials, including hardness, tensile strength, fatigue resistance [131–134], wear resistance [135], and corrosion resistance [136]. The process facilitates grain refinement [137–139], defect elimination [140, 141], dispersion of reinforcement particles, and the incorporation of alloying elements without necessitating welding [138]. Additionally, FSP has demonstrated its effectiveness in processing various materials, including aluminium alloys [142, 143], titanium alloys [144–149], magnesium alloys [150, 151], and dissimilar or composite materials [146, 152–154]. Moreover, FSP has proven its effectiveness in superplasticity of aluminium alloys. Superplasticity means increasing the uniform elongation ability of any metallic material by more than 200% prior to failure. A detailed summary of previously reported superplasticity in all aluminium alloys using FSP is summarised in [155]. Furthermore, FSP has demonstrated high fabrication performance for in-situ Aluminium Metal Matrix Composites (AMMCs), which are considered among the fastest-developing materials for structural applications, as summarised in [143].

Several methods are available for incorporating reinforcement particles into the material during FSP. One common approach is the use of a cover plate, often referred to as the "sandwich" method, where the particles are placed between two layers of material before the processing begins. Another technique is the groove method, where a groove is machined into the material surface and filled with reinforcement particles before FSP is performed. The hole method involves drilling holes into the material, filling them with reinforcement particles, and then applying FSP to disperse the particles uniformly within the matrix [15]. These methods, illustrated in Fig. 12, enable precise control over the distribution and concentration of reinforcement particles, leading to tailored improvements in the material's microstructure and properties.

As previously discussed, FSP is derived from FSW and, therefore, shares several parameters that similarly influence its outcomes. In this section, we will review studies that examine key parameters such as the number of passes, tool path trajectory, and pin shape. Additionally, various research efforts have explored strategies to enhance FSP performance, including the use of cooling systems, stationary shoulder tools, and the application of hybrid techniques. Furthermore, we will examine the impact of FSP on surface modification and the enhancement of surface hardness. This is achieved through improved microstructural and compositional homogeneity, as well as effective grain refinement, using composite powder materials across various alloys, including both heat-treatable and non-heat-treatable aluminium alloys.

The FSP groove filling method was utilised by Mathur et al. [156] to reinforce aluminium alloy AA5052 with titanium dioxide (TiO2) nanoparticles using a 6 mm square pin length. The study considered input parameters such as groove width, rotational speed, and traverse speed. The examination revealed a fine mixing of the TiO2 nanoparticles with the base material in the grain structure. The findings demonstrated enhancements in the hardness value and tensile strength of the base material attributed to the uniform distribution of the TiO2 nanoparticles. Figure 13 illustrates the uniform distribution of elements in the FS-processed region. Selecting optimal parameters, such as the number of passes, plunge depth, and pin shape, is crucial for enhancing the microstructural and mechanical properties of FSP. The impact of multi-passes FSP on wear performance and microstructure of titanium grade 2 was investigated by Vakili-Azghandi et al. [157]. Their findings revealed that multi-pass FSP improved wear resistance and surface hardness, driven by grain size reduction and the development of a strong texture with a high percentage of high-angle grain boundaries. Meanwhile, the pin shape parameter was

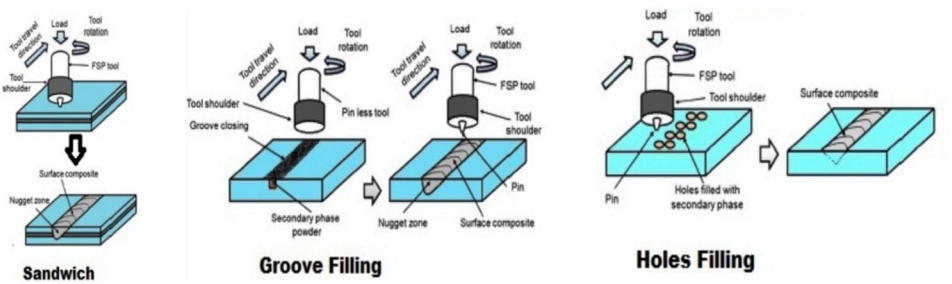

Fig. 12 Addition methods of reinforcement particles in FSP [15]

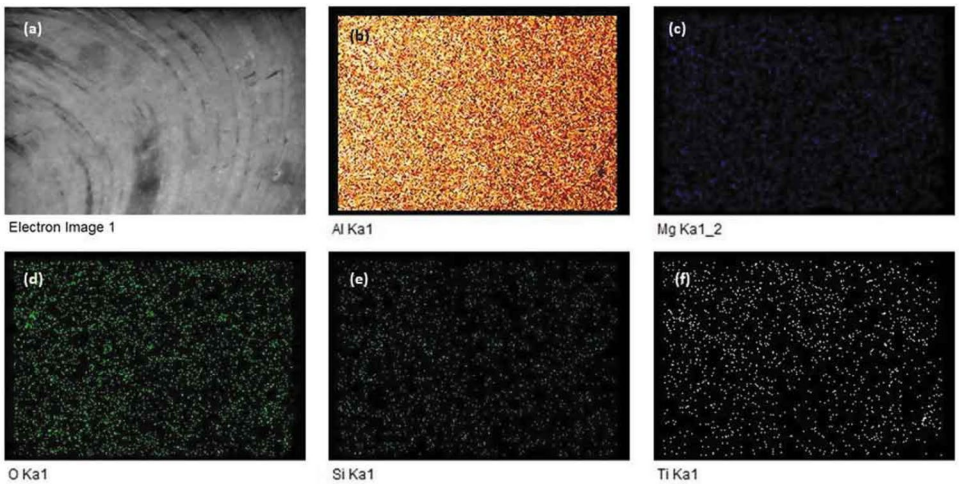

Fig. 13 **a** SEM of FSPed area. Uniform distribution of (**b**) aluminium, (**c**) magnesium, (**d**) oxygen, (**e**) silicon and (**f**) titanium in the region [156]

investigated in the study by Patel et al. [158]. They explored the effect of different pin shapes- square, pentagon and hexagon- on 7075 aluminium. They found that the square pin profile produced the highest temperature (400 °C), superior stir zone hardness, and a fine grain structure without defects, outperforming other shapes. However, further investigations are required to elucidate the underlying mechanisms behind the observed improvements and optimize a broad spectrum of process parameters for specific applications. Zhang et al. [159] included the effect of plunge depth in their study and used FSP to enhance the ductility and yield strength of high-nitrogen stainless steel (HNS). Their study demonstrated a significant enhancement in yield strength, which increased from 540 to 1300 MPa after 50% cold rolling. However, post-FSP, the yield strength decreased to 950 MPa with improved elongation and increased hardness in the stir zone. Additionally, the study highlighted the influence of plunge depth on tensile properties, which showed that higher plunge depths led to a noticeable decrease in elongation. In contrast, lower plunge depths resulted in less effective improvement of yield strength.

The documented reports emphasise the critical role of FSP process parameters, including groove filling, multi-pass operations, pin shape, and plunge depth. Each parameter affects material properties differently, such as hardness, tensile strength, wear resistance, and grain structure. These findings underscore the importance of optimising process conditions to achieve desired enhancements in various materials while also indicating the need for further research to fine-tune these parameters for specific applications. Further investigation on the effects of tool geometry can be found in [91].

Various studies have delved into strategies aimed at enhancing performance, including the utilisation of cooling systems, stationary shoulder tools and the application of hybrid techniques. The cooling system plays a crucial role in determining the microstructural evolution of processed materials, as it controls the temperature distribution during processing. This temperature management directly influences grain size and, consequently, the overall performance of the material. Ralls et al. [160] employed FSP on cold-sprayed 316L stainless steel deposits to improve their tribological and corrosion behaviour. Their study revealed that FSP induced an austenitic phase transformation. After FSP, the wear rate and friction of the cold-sprayed deposit were reduced by 55.1% and 8.3%, respectively. These enhancements were attributed to pore closure and grain refinement. Additionally, after combining cold spraying with heat treatment through FSP, the corrosion rate decreased by approximately 35%, while the pitting corrosion resistance enhanced by around 27%. Another study aimed to reduce heat input during FSP without external cooling by using a stationary shoulder tool with a rotating probe was carried out by Patel et al. [161]. Unlike traditional FSP tools, a stationary shoulder generates less frictional heat; hence, the shoulder contributes little deformation at the top surface during processing. This approach generated a small temperature gradient across the 6.35 mm thick AZ31B magnesium alloy. The results showed an enhancement in hardness and a refined grain structure throughout the material's thickness, including the top, middle, and bottom layers. Hybrid FSTs effectively combine the benefits of different processes to enhance material properties. This is for the repair of pores formation during wire-arc additive manufacturing (WAAM) and the enhancement of process outputs. He et al. [162] studied a hybrid method integrating wire-arc additive manufacturing (WAAM) with FSP to improve the fatigue properties of AA4043 aluminium alloy, using AA6082-T6 as the substrate. FSP was applied after every three WAAM layers, resulting in a significant improvement in fatigue performance and ductility, though with a 9.8% reduction in UTS. However, elongation at failure increased by 108.7%. These

results are consistent with other studies, such as [163], which also showed improvements in Al-4043 alloy components via friction stir post-processing. Another study was carried out by Kalashnikova et al. [164] to investigate the multi-passes impact in a hybrid technique combined with wire-feed electron beam AM with FSP to enhance the mechanical properties of AA4130 and AA5056 aluminium alloys. Mabuwa et al. [165] applied FSP to TIG-welded joints of AA8011 and AA6082 alloys. While the hardness of TIG-welded joints was higher than that of FSPed TIG-welded joints, tensile strength slightly increased from 83.83 MPa to 90.09 MPa after FSP. Significant material mixing and reduced grain sizes were also observed, highlighting the potential of hybrid FSTs to refine microstructure and mechanical properties. These studies collectively demonstrate that hybrid FSTs, particularly when combined with additive manufacturing processes like WAAM, can enhance mechanical properties and microstructural characteristics, albeit with some trade-offs in certain areas like tensile strength.

Collectively, these studies highlight the effectiveness of cooling systems, stationary shoulder tools, and hybrid FSTs in enhancing material properties and microstructural characteristics. However, the trade-offs, such as reduced tensile strength or the need for further research into long-term durability and practical applicability, suggest that additional investigations are required to understand and optimise these techniques for real-world applications fully.

FSP is highly effective for surface modification and enhancement of surface hardness. It is versatile in its application, as both the metal matrix and the reinforcement material (particulate) can be either ferrous or non-ferrous and can be compatible or non-compatible. FSP has been employed to fabricate various types of composites, including surface composites, nanocomposites, in-situ composites, and hybrid composites. Additionally, research has explored the use of composite materials in FSP to improve the joint quality of aluminium alloys, demonstrating the technique's broad applicability and potential for material property enhancement. Nazari et al. [51] applied both hybrid and single-surface composites to AA6061 using FSP, incorporating nano-sized graphene (0.5–2 wt%) and micro-sized TiB2 (10–30 wt%). They found that these particles refined the grain size to less than 1 µm in the SZ, thereby enhancing the hardness and tensile properties, with the optimal mix being 1 wt% graphene and 20 wt% TiB2. Similarly, Sharma et al. [166] utilised mono (B4C) and hybrid (B4C + MoS2) powders to develop surface composites in AA6061 aluminium alloy. The study employed multi-pass FSP with different directional strategies, resulting in a uniform distribution of reinforcement particles without clustering in the processing zone. The highest hardness was achieved with the mono (B4C) surface composite, while using ($75\%B_4C + 25\%MoS_2$) improved wear resistance due to the solid lubricant properties of MoS2. Barati et al. [167] reinforced AA6061 using SiO2 nanoparticles via FSP, with and without vibration. Calcium carbonate (CaCO3) was also used in AA6082 composites, where the grain size was reduced to 10–12 µm due to dynamic recrystallisation, significantly improving microhardness and wear resistance [168]. Vanadium particles were introduced into AA6063 through FSP, which enhanced tensile properties while maintaining ductility due to uniform particle dispersion and fine-grain structure [52]. In another study, Deore et al. [169] aimed to enhance the surface of AA7075 by comparing different filler materials—Silicon carbide (SiC), Copper (Cu), and Multiwall carbon nanotubes (MWCNT)—during FSP. They found that FSP induced grain refinement with all fillers, with SiC achieving the finest grain size. Post-process age hardening produced MgZn2 precipitates, improving impact toughness, microhardness, and wear resistance. Kumar et al. [170] found that adding niobium carbide (NbC) particles also enhanced the hardness and tensile strength of FSPed AA7075. These studies have shown that incorporating composite materials into aluminium alloys using FSP improves mechanical properties. Techniques involving nano-sized graphene, TiB2, SiO2, CaCO3, and vanadium particles lead to grain refinement and enhanced hardness, tensile strength, and wear resistance. Comparative studies on AA7075 with various fillers revealed that materials like SiC and MWCNT significantly improve microstructural properties, while post-process treatments further optimise performance.

These studies collectively demonstrate that incorporating various composite materials into aluminium alloys via FSP leads to significant improvements in mechanical properties, including grain refinement, hardness, tensile strength, and wear resistance. Techniques involving nanoparticles and different fillers consistently enhance microstructural and property characteristics, with additional post-process treatments further optimising performance. For a deeper understanding of FSW in dissimilar heat-treatable aluminium alloys, refer to studies [171] and [172].

Other studies have explored the effects of composite powders on the microstructure and properties of non-heat-treatable aluminium alloys. Akinlabi et al. [173] explored the application of FSP to create surface composites of AA1050 reinforced with TiC powder. They examined how rotational speeds (1200 and 1600 RPM) and traverse speeds (100, 200, and 300 mm/min) impacted the microhardness and wear resistance of the resulting Al-TiC composites. The TiC powder was compacted into a V-groove on the material surface using a pinless tool, with the optimal parameters identified as 1200 RPM and 100 mm/min, resulting in effective heat generation and TiC powder melting. Similarly, Zhang et al. [174] studied the effect of heat input on the microstructure and mechanical properties of Al1060 nanocomposites reinforced with carbon nanotubes

(CNTs). By varying rotational speeds (600, 750, and 950 RPM) and traverse speeds (30, 95, and 150 mm/min), they found that increased energy input led to slight grain coarsening and better CNT dispersion within the Al1060 matrix. The highest energy input significantly enhanced the mechanical properties, resulting in a 53.8% increase in tensile strength and a 31.2% increase in elongation compared to unreinforced aluminium. Sathish et al. [175] reinforced AA8006 aluminium alloy with zirconium dioxide (zirconia) using FSP. The study found that zirconia improved weld quality, with rotational speed affecting corrosion resistance, surface grain structure, tensile strength, and microhardness in the welded zone. Further research by Jain et al. [176] explored the incorporation of TiO2 particles into AA1050 using FSP. They investigated the effect of multiple FSP passes, with alternating directions between passes. Their findings showed that while the first pass resulted in particle agglomeration and insufficient material flow, the second pass produced a more uniform microstructure with finer grains and improved hardness. These results were consistent with those of another study [53], which analysed the effects of multiple FSP passes using Al2O3 nanocomposites with AA1050. Overall, these studies underscore the importance of processing parameters in optimising the microstructure and mechanical properties of aluminium-based composites.

Overall, these studies highlight the significant role of processing parameters in optimising the microstructure and mechanical properties of aluminium-based composites. They demonstrate that careful control of FSP parameters can effectively enhance the performance of non-heat-treatable aluminium alloys through improved reinforcement distribution, grain refinement, and property enhancement.

In summary, FSP shares the fundamental principles of frictional heat generation and plastic deformation with FSW. However, FSP is applied differently to achieve specific objectives in enhancing the mechanical and microstructural properties of materials. While FSP offers notable benefits, including improved material properties without melting, it also presents challenges, such as the formation of a keyhole defect and the requirement for a suitable fixture to hold the workpiece in place during processing.

2.5 Friction Surfacing (FS)

Friction surfacing (FS) is a surface-coating process derived from FSP. Unlike FSW and FSP, FS utilises a consumable tool that is plastically deformed and traverses across the workpiece [177]. This tool, subjected to high rotational speed and forging force, generates frictional heat, softening both the rod material and the substrate. As a result, they bond together, forming a deposited layer on the substrate

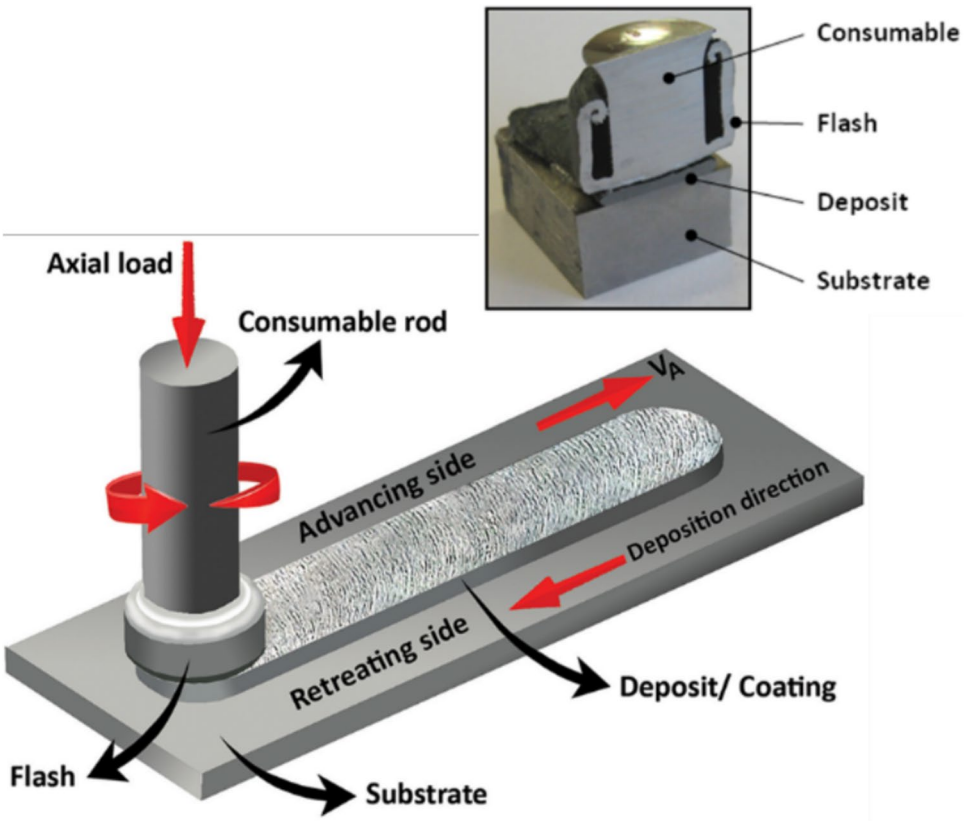

Fig. 14 Friction surfacing process [178]

surface [178], as depicted in Fig. 14. This layer enhances the mechanical, tribological, and corrosion properties of the substrate [179].

Optimising FS process parameters affects the temperature distribution and the coating thickness of the tool material. Kallien et al. [180] delved into the effects of FS process parameters on temperature profiles and deposition geometry when applying an AA 5083 H112 rod onto an AA 7050 T7451 substrate. Key parameters examined included axial force, rotational speed, and traverse speed. Their findings highlighted the significance of tool rotational speed and axial force in influencing temperature dynamics. Specifically, they noted a direct correlation between rotational speed and temperature development. Moreover, higher axial force resulted in the formation of thinner and wider deposits. The study also revealed that substrate thickness played a role in temperature distribution, with the use of a Ti backing plate maintaining temperature better than an Al backing plate, leading to thinner and wider deposits. Yu et al. [181] employed an AA6061 aluminium alloy rod with a diameter of 20 mm to coat a 2 mm thick Q235 plate substrate using FS. Rotational speeds of 1400, 1600, and 1800 rpm were applied. Their investigation revealed a significant influence of rotational speed on the dimensions of the coating layer. The maximum deposition thickness of 5 mm was achieved at 1600 rpm, exhibiting better corrosion resistance, randomly distributed intermetallic compounds (IMCs), and a refined microstructure. Conversely, rotational speeds of 1800 rpm and 1400 rpm yielded deposition thicknesses of 1.5 mm and 1.2 mm, respectively. These findings align with those of previous studies [179, 182–184]. Other techniques were explored to investigate the FS performance by incorporating particle reinforcement. Pirhayati and Aval [185] employed a consumable AA2024 aluminium alloy rod with a diameter

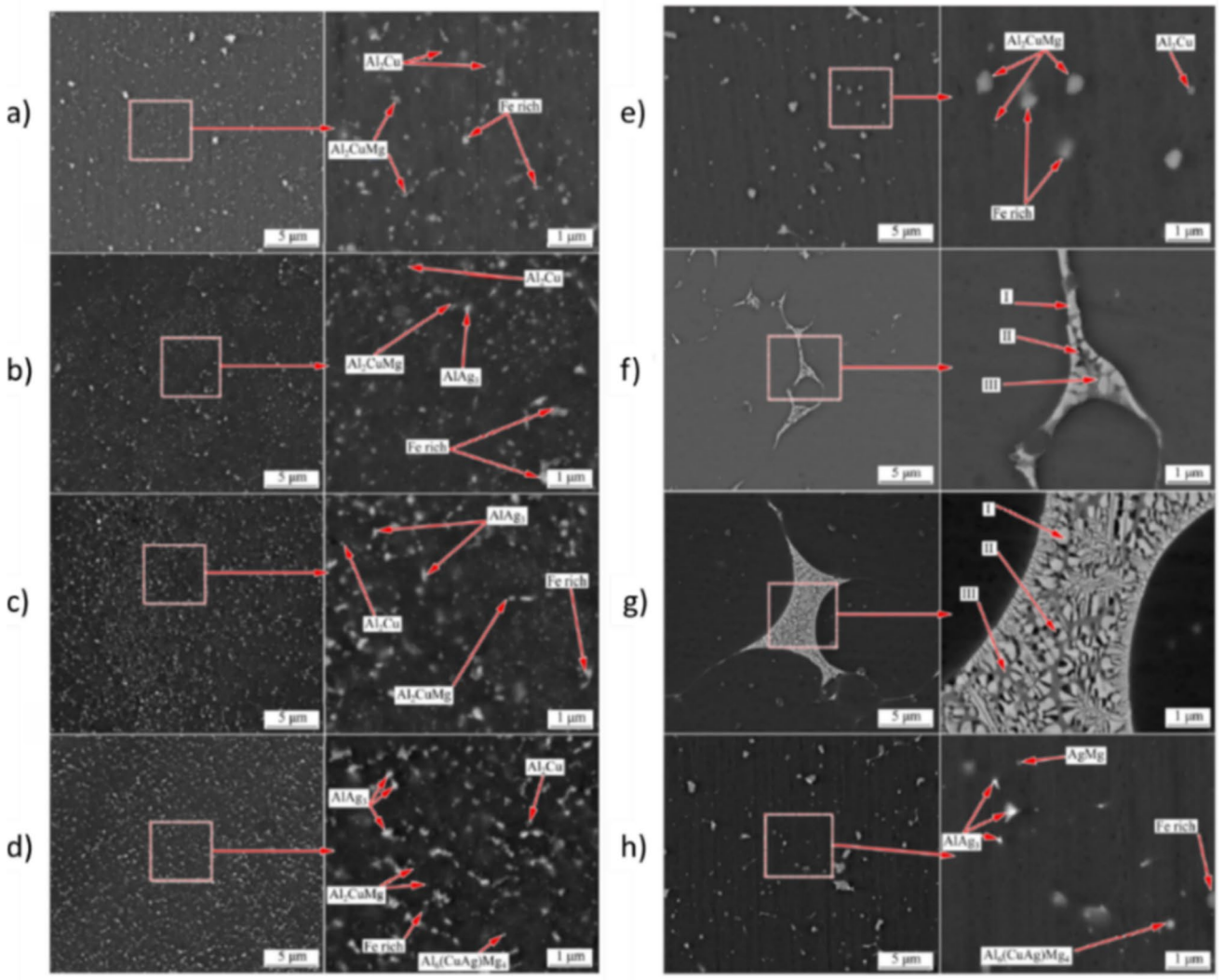

Fig. 15 SEM images of coated samples (a-d) before heat treatment and (**e–h**) after heat treatment: **a-e** 0 wt.% Ag, (**b-f**) 5.3 wt.% Ag; **c-g** 10.6 wt.% Ag; **d-h** 16.0 wt.% Ag

of 20 mm, featuring drilled holes for feeding silver (Ag) particles at concentrations of 5.3, 10.6, and 16 wt.%. These particles were introduced during the coating process of a 2 mm thick AA2024 aluminium alloy substrate. Their findings indicated a decrease in coating efficiency with the addition of small amounts of Ag powders. Moreover, the grain size of the coating was reduced due to the formation of a solid solution of Al – Ag and intermetallic compounds containing Ag. Figure 15 represents the SEM images of coated samples before and after heat treatment at different concentrations of Ag. Bararpour et al. [186] employed a similar technique by introducing zinc powder through drilled holes in a 20 mm diameter Al–Mg alloy consumable rod. They utilised an AA5052 aluminium alloy plate with a thickness of 2 mm as the substrate material. Their study revealed that the presence of Zn powder enhanced the thermal stability of the coating. Additionally, the kinetics of grain growth during heat treatment decreased from 1.46 mm/h for coatings free of Zn to 0.55 mm/h for coatings containing Zn. Moreover, they observed an increase in the strength and hardness of the Zn-containing coating after 8 h of heat treatment, but this effect decreased after 12 h. There is a lack of exploration into the optimal particle concentrations or types for enhancing coating properties. Moreover, there is limited research on the performance of the hybridisation of FS with external energy sources.

In summary, FS has found extensive application in both low and high-melting-point alloys, including aluminium, magnesium, titanium, and steel-based alloys [187]. Moreover, FS has demonstrated superior performance in coating both similar and dissimilar materials compared to other cladding methods. However, FS has some disadvantages, such as poor bonding at edges and the presence of a revolving flash around the rod, which contributes to a decrease in the deposited mass [188].

2.6 Additive Friction Stir deposition (AFSD)

Additive Friction Stir deposition (AFSD) is another technique based on additive manufacturing, such as FSAM, which emerged with a patent in 2016 [9]. Unlike FSAM, AFSD is not grounded in welding concepts but rather focuses on a solid-state processing approach that harnesses the advantages of additive manufacturing. The AFSD process merges the flexibility inherent in additive manufacturing with the robust material properties characteristic of solid-state processing techniques [126, 189]. This method is applied across various industries, including aerospace, automotive, and general manufacturing, where there is a demand for high-strength, high-quality components [190, 191]. Additionally, AFSD offers an innovative solution for recycling waste metals by utilizing metal chips as the deposition material [192]. The technique provides versatility through three primary methods: using feedstock directly, feeding powder through the tool, or placing the powder in front of the tool, as illustrated in Fig. 16 [16]. Each approach allows for different applications and customization of the deposition process, making AFSD a flexible and efficient technology for both new manufacturing and material recycling.

In AFSD, a hollow rotating non-consumable tool generates frictional heat. This heat softens the supplied material—either feedstock or powder—which is then deposited layer by layer onto the substrate. Recrystallisation in the deposited area leads to the formation of fine grains [189].

For the feedstock method, Anderson-Wedge et al. [193] conducted a parametric study to explore the influence of rotational speed (ranging between 175 and 300 rpm) and traverse speed (ranging between 88.9 mm/min and 139.7 mm/min) of the AFSD tool. The material was deposited as a square rod through the hollowed tool, with a feedstock feed rate of 78.74 mm/min for 175 rpm, and 101.6 mm/min and 88.9 mm/min for the remaining experimental runs. To promote material mixing, a tool with four protrusions on the tool face was employed. The optimal parameters were identified as 200 rpm and 101.6 mm/min, and the resulting microstructural properties were compared with those of AA2219-T87. The grain size of the AFSD part was approximately 5.5 times smaller than that in AA2219-T87, as illustrated in Fig. 17. Due to the monotonic and cyclic strain-controlled response, the accumulation of the AFSD part was

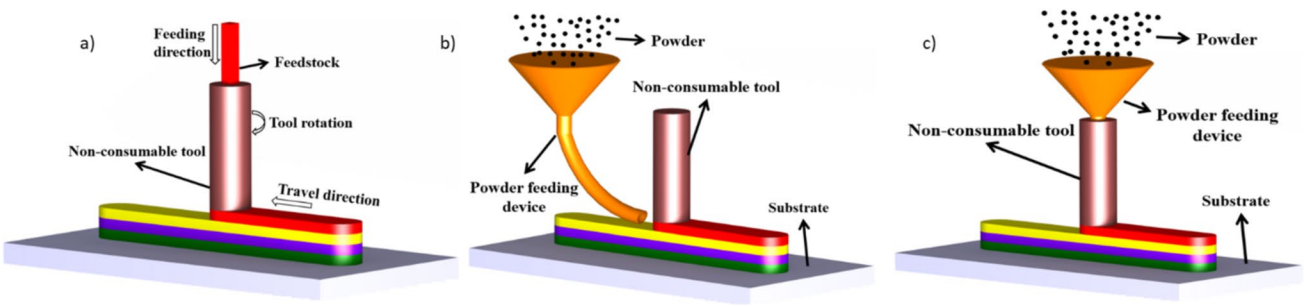

Fig. 16 AFSD process types: **a** feedstock, (**b**) feeding powder in front of the tool, and (**c**) feeding powder through the tool [16]

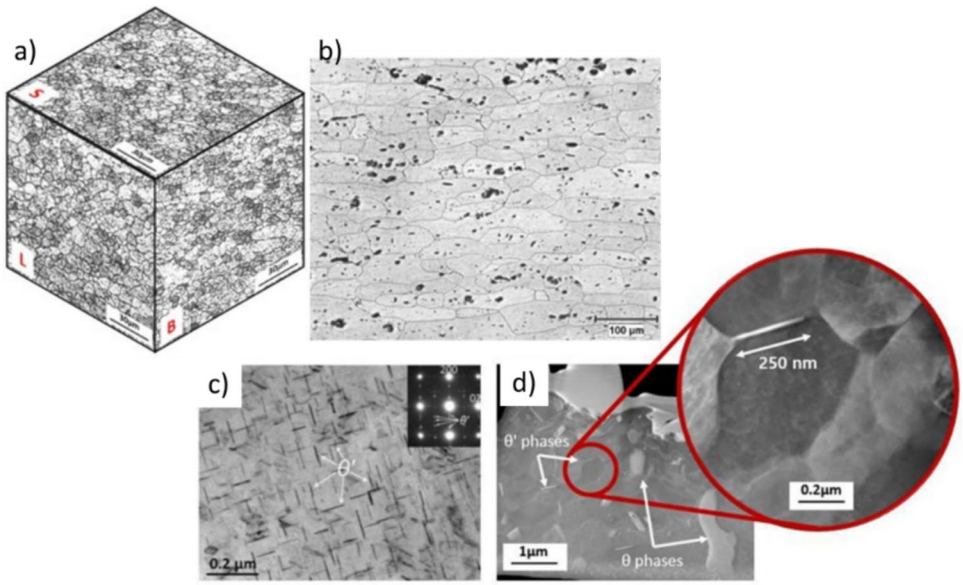

Fig. 17 Optical macrostructure represents the grain sizes of (**a**) AFSD AA2219 and (**b**) wrought AA2219-T87, and TEM micrographs of (**a**) wrought AA2219-T8 and (**b**) as-deposited AA2219 illustrating θ and θ' precipitates [193]

slower than that of the wrought material. Garcia et al. [194] conducted a parametric study to investigate the influence of the AFSD tool's rotational speed (300, 600, and 900 rpm) and traverse speed (1.00, 2.00, and 3.00 mm/s) on temperature evolution and heat generation. Two different materials were investigated: pure copper (Cu) and AA6061 aluminium alloy, with both the deposited material and substrate being of the same composition. The interfacial contact was observed under partial slipping/sticking conditions for AA6061 and full slipping conditions for Cu. Consequently, we observed differences in heat generation between AA6061 and Cu, which led to variations in the power laws governing peak temperature. These results are consistent with [195, 196].

Several studies have explored the utilisation of powder materials. For instance, Derazkola and Simchi [197] employed AFSD to fabricate polycarbonate-based nanocomposites by injecting colloidal alumina nanoparticles into a plasticised polymer. The process parameters included a rotational speed of 2000 rpm, a traverse speed of 30 mm/min, a plunge depth of 0.4 mm, and a tilt angle of 2 degrees. Colloidal nanoparticles were fed using a screw extrusion system rotating at the same speed as the tool. SEM analysis revealed a laminar flow of the polymer with a small accumulation of nanoparticles due to in-situ feeding, resulting in significant changes in the physicomechanical properties of the polymer. The tensile strength and hardness in the longitudinal direction were observed to be approximately 26% and 9% higher, respectively, than those in the transverse direction. Crack propagation was observed from the heat-affected zone (HAZ) to the stir zone (SZ) interface. Mukhopadhyay and Saha [198] conducted a layer-by-layer deposition of a 7 mm thickness of pure aluminium powder with particle sizes ranging from 50 to 300 µm using AFSD. Employing an H13 concave bottom probless tool, the study involved initial groove application on the substrate to aid deposition and minimise powder dispersion during the process. The powder was fed through a duct from a container positioned ahead of the AFSD tool. They observed no discernible microstructural differences between the transverse and short-transverse directions. Furthermore, they noted an

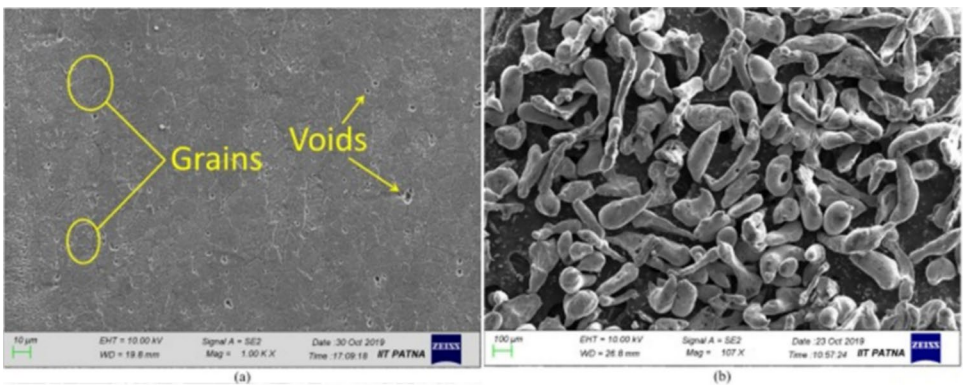

Fig. 18 SEM image of (**a**) deposit and (**b**) aluminium powder [198]

improvement in the deposited powder tensile strength compared to strain-hardened AA1060-H12 (pure aluminium). In contrast to FSAM, they concluded that AFSD deposition did not directly influence the microstructure of the previously deposited layer, attributed to the probe-less nature of the AFSP tool, which did not penetrate the layer for stirring. Figure 18 represents an SEM image of the deposit and aluminium powder. Jordon et al. [199] investigated the impact of AFSD on recycling waste machine chips of AA5083-H131 aluminium alloy. They utilised the chips as feedstock fed through the AFSD tool. Electron backscatter diffraction analysis revealed an equiaxed grain structure with a diameter of 1.5 mm. Their findings suggest that AFSD holds promise for recycling machine chips to produce dependable structures. However, there is a lack of comparative studies between AFSD-produced parts and conventionally manufactured counterparts, which could provide valuable insights into the advantages and limitations of the AFSD process.

These studies illustrate the potential of AFSD for a variety of applications, including the enhancement of polymer properties with nanoparticles, the deposition of aluminium powders, and the recycling of aluminium waste. Further research is necessary to compare AFSD-produced parts with conventionally manufactured counterparts and gain a better understanding of the long-term performance and durability of AFSD-fabricated components, even though AFSD shows promise in improving material properties and enabling recycling.

In summary, the AFSD process offers numerous advantages, including homogeneous microstructural characteristics, excellent mechanical properties, and the absence of melting, which helps reduce residual stress [200]. These attributes have led to its application in various industrial settings. Some notable applications of AFSD include recycling waste chips into products [199, 201], reinforcing automotive panels [202], and facilitating the structural repair of components [203, 204]. Additional research on AFSD can be explored in [205].

3 Hybrid FSW processes

As previously mentioned, FSW is considered the foundational technique among FSTs and sharing many principles with other FST methods. This section focuses on enhancement approaches applied to FSW, particularly through the integration of external energy sources.

Despite the proven advantages of FSW over traditional fusion welding techniques, several challenges remain, particularly when welding materials with intermediate to high tensile properties and higher melting points. These materials include high-strength aluminium alloys, ferrous metals, titanium, nickel, and copper alloys, as well as metal matrix composites. The primary challenge lies in generating enough heat to effectively soften these materials during welding [206]. Consequently, numerous studies have focused on optimizing FSW process parameters to identify the optimal conditions that produce adequate frictional heat for softening the materials near the weld region. Additionally, effective heat generation not only reduces the load on the welding tool but also enhances tool life, welding efficiency, and overall weld quality.

Other attempts have been carried out to address the limitations of FSW in welding harder materials, including hybridizing the FSW process with external energy sources that provide additional preheating or pre-softening mechanisms [82]. These external energy sources can be classified into thermal and mechanical energy sources. Thermal energy sources, such as induction [207], laser [208], electricity [209], arc [210], and plasma [211], apply heat to the workpieces, facilitating material softening before or during welding. In contrast, mechanical energy sources, like ultrasonic vibration [212], enhance material flow during the FSW process without significantly altering the process temperature.

This hybridization approach aims to overcome the challenges posed by harder materials and improve overall welding performance. This part will talk about different hybrid FSW processes, such as induction-assisted FSW, laser-assisted FSW, electrically-assisted FSW, arc-assisted FSW, and ultrasonic vibration-assisted FSW. We will talk about how they work and how they have helped the FSW technique move forward.

3.1 Induction-assisted FSW

Induction heating is a well-known and widely used method for heating and heat-treating materials, particularly steel. This technique offers several advantages, including rapid and precise localised heating, environmental friendliness, and lower energy consumption compared to other heating methods. The principle of induction heating involves interactions among thermal, electromagnetic, and metallurgical phenomena. An alternating electric current generates an electromagnetic field, causing eddy currents within the workpiece. The material then distributes the generated heat from these eddy currents. The amount of energy produced depends on the material's properties, such as its electrical conductivity and magnetic permeability [213].

Leveraging the advantages of induction heating, researchers have developed a technique to enhance FSW by integrating it with induction heating, resulting in what is known as induction-assisted friction stir welding (IaFSW). As shown in Fig. 19, IaFSW uses a non-contact electromagnetic induction source, a coil carrying an alternating current, to heat the conductive material. When the coil introduces this material

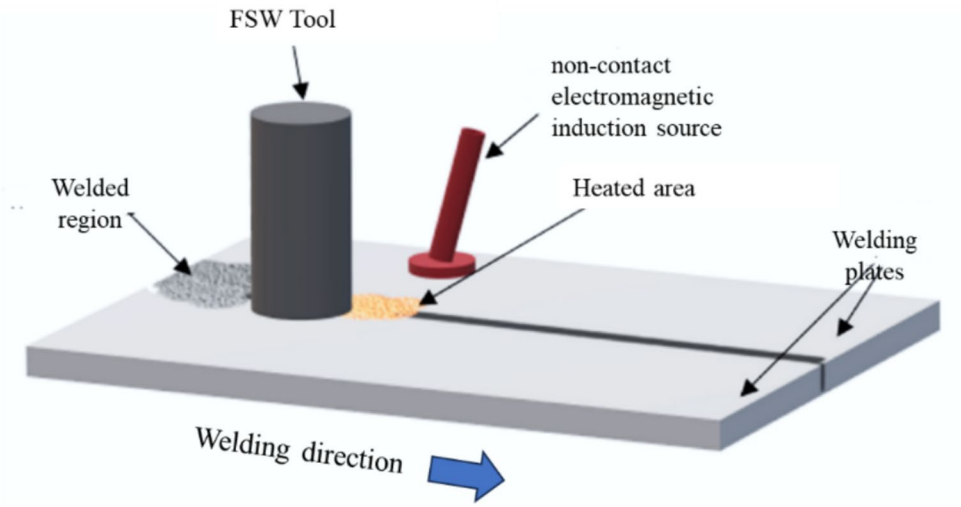

Fig. 19 Induction-assisted FSW process [36]

into its magnetic field, the resistance to the current flowing through it causes it to heat up. We apply this heating source to preheat high-melting-point materials or the FSW tool. IaFSW has demonstrated several advantages, including increased welding speed, reduced welding forces, and enhanced microstructure of the welded joint [206, 207].

Saha and Biswas [214] conducted a comparative study between FSW and IaFSW. This study used the Inconel 718 alloy and evaluated the temperature distribution and residual stresses. The findings indicated a 15% decrease in residual stresses in IaFSW joints compared to FSW. Moreover, the temperature was uniformly distributed in IaFSW, experiencing an increase of 138 °C. Finite element modelling revealed a 23% reduction in reaction forces on the pin during plunging in IaFSW, and plastic strain values in IaFSW were 55% higher than those in FSW. According to the same authors [215], increasing the traverse speed in IaFSW resulted in a sound welded joint for Inconel 718 alloy. Raj and Biswas [216], conducted another comparative study between FSW and IaFSW. They made different joints with Inconel 718 and stainless steel (SS316L) alloy, moving at 70 mm/min in FSW and 140 mm/min with induction heating at 300 °C in IaFSW. Both welding techniques resulted in highly refined grains, as shown in Fig. 20. The findings indicated that the I-FSW process could produce high-quality joints at elevated traverse speeds. Additionally, preheating reduced the downward force and enhanced tool life. In an attempt to eliminate the presence of exit holes in FSW, Ramon et al. [217] employed a billet with a volume similar to that of an exit hole. They investigated the efficacy of an induction heating source for eradicating this defect. Utilising a two-dimensional numerical simulation, the researchers analysed the influence of IaFSW on AA1100. The results indicated that IaFSW demonstrated notable efficacy in rectifying the exit hole defect.

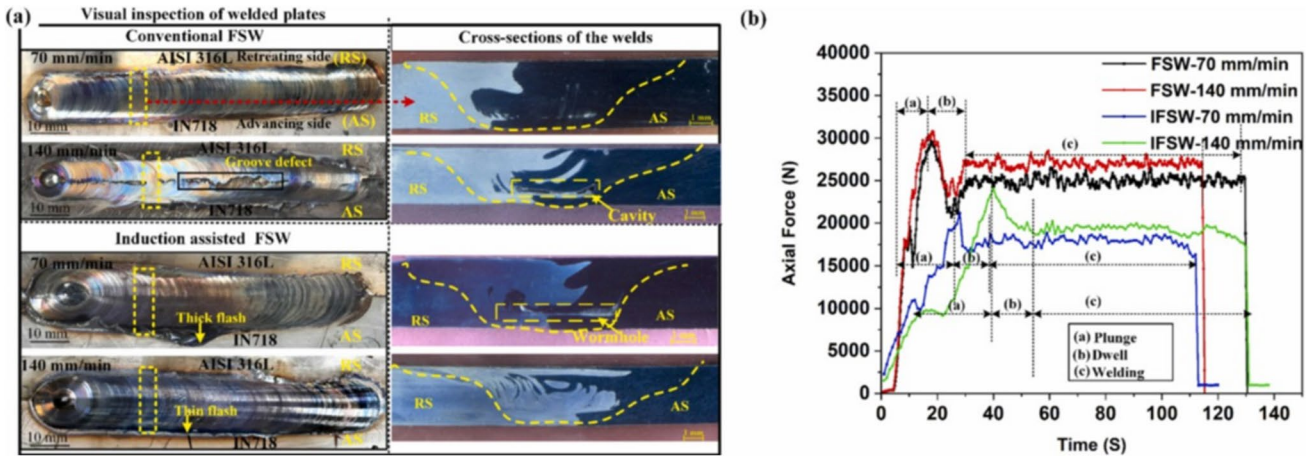

Fig. 20 **a** Visual inspection and cross-sectional views of welded plates and (**b**) Axial force diagram during the FSW and I-FSW [216]

Collectively, these studies illustrate that IaFSW not only enhances the mechanical properties and performance of welded joints but also provides solutions to common defects, offering a valuable alternative to traditional FSW methods. However, utilising IaFSW has limitations [206, 207]. This technique applies to electrically conductive materials. Additionally, it is challenging to ensure that the heating is precisely directed to the intended position and that control measures are necessary to prevent undesirable sparks and potential electrical shocks [82, 207].

3.2 Laser-assisted FSW

Laser welding is a highly precise fusion welding technique that leverages a focused laser beam to melt and join materials. This technique involves directing a high-intensity laser beam onto the workpieces using mirrors or optical lenses to concentrate the heat at a specific location. Commonly used laser sources for this process include CO2, ytterbium fiber, and multimode Nd: YAG lasers [218]. Laser welding is noted for its exceptional precision and accuracy, as it can concentrate the beam on a small area, leading to minimal thermal distortion and improved control over the weld quality. The method is both rapid and effective, making it suitable for high-precision applications.

Laser-assisted friction stir welding (LaFSW), illustrated in Fig. 21, integrates the principles of laser welding with FSW to enhance performance. In LaFSW, the laser beam is employed to preheat the workpiece material prior to the engagement of the rotating pin of the FSW tool. This preheating step helps to soften the material, thereby facilitating the welding process. The application of laser preheating significantly improves the efficiency of the FSW process, leading to enhanced weld quality, increased productivity, and reduced overall welding time [219]. By combining these two technologies, LaFSW addresses some of the limitations associated with traditional FSW, such as difficulties in welding high-melting-point materials and achieving optimal weld characteristics. This hybrid approach thus represents a significant advancement in welding technology, offering greater flexibility and effectiveness across a range of materials and applications.

Wada et al. [220] investigated the preheating impact of laser power and laser position on the FSW process torque and defect formation during the welding of carbon steel (S55C). The laser source was maintained at an irradiation angle of 45°, with a power range varying between 1000–2000 W. Results from the study indicated that defect-free joints were achieved when applying the laser source at the retreating side with a laser power exceeding 1500 W. It was elucidated that the LaFSW technique reduced torque and resisting force on the tool compared to traditional FSW. Additionally, the study highlighted that the laser source position influenced the characteristics of the welded joints. Two fully coupled thermomechanical numerical simulation models were employed by [221] using Abaqus/Explicit to explore the impacts of FSW and LaFSW. In this investigation, the laser source was positioned at a 20 mm distance from the rotating tool. Through optimising process parameters, the researchers determined that the traverse speed in LaFSW could be increased to 1500 mm/min, producing high-quality joints in low alloy steel grade DH36. Furthermore, they observed that the axial force in LaFSW was approximately half that in FSW, leading to an extended tool life and improved process efficiency. The post-heating process effect using laser peening (LP) was investigated by [222] through a combination of a 3D finite element model implemented in ABAQUS software and experimental work. The study focused on applying LP to an FSWed joint of Al-Li 2195 alloy to examine its impact on residual stress distribution. Key input parameters included laser power density, impact number, and spot overlap. The findings revealed a direct proportionality between residual stress and laser power density, laser impact number, and an inverse proportionality with spot overlap rate.

Despite the advantages of LaFSW over IaFSW, several challenges remain. Campanelli et al. [208] identified that

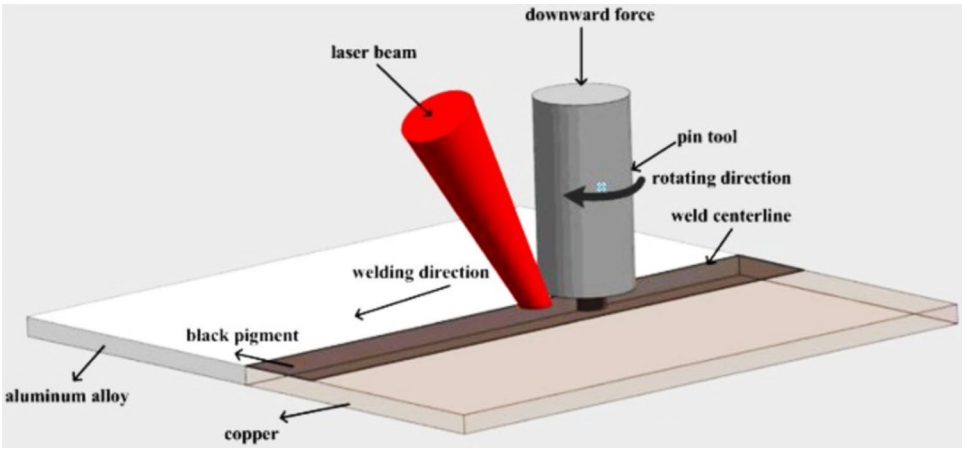

Fig. 21 Laser-assisted FSW process [219]

LaFSW is significantly more expensive and tends to have higher power consumption compared to IaFSW. Furthermore, the use of any external heating source in conjunction with FSW introduces the risk of overheating. This can lead to several issues, including melting of the workpiece, formation of liquified cracks, and an increased size of the HAZ [219, 223]. These drawbacks underscore the need for careful management of the heating parameters to mitigate potential negative impacts on weld quality and overall process efficiency.

3.3 Electrically-assisted FSW

Electrically assisted friction stir welding (EaFSW) operates on the principle of generating resistance heating in the welding zone through the flow of electric current. An external power supply is employed to produce the required electrical current. A mica film is utilised in the backing plate to insulate the workpiece. A cooling system is required to prevent pin damage due to excessive current [224]. However, certain precautions must be taken when using EaFSW, including the need for insulating and cooling systems [82]. An AC power supply is preferred over a DC power supply in EaFSW because it provides a more uniform energy distribution. This is attributed to the cyclic nature of tool rotation and the uniform sinusoidal waveform of energy [82, 224]. EaFSW may lead to a root defect that is challenging to detect through non-destructive testing. This defect can result in failures in structures exposed to corrosive environments, such as those in naval or aerospace applications [82].

As illustrated in Fig. 22, the EaFSW process can be categorised based on the electrical current circuit. In this configuration, the FSW is connected to the positive side of the power supply, while the conductive strip can be positioned at the back of the workpiece (Fig. 22-a). The generated resistance heat acts as a heat treatment to reduce the residual stresses in the welded joint as the current passes behind the welding tool [209]. Alternatively, if the conductive strip is connected to the front of the workpiece (Fig. 22-b), this process is referred to as a preheating process, softening the metal along the joint line. This connection is suitable for hard materials as it reduces welding forces and extends the life of the FSW tool [225]. The third model, depicted in Fig. 22-c, is applied when welding dissimilar materials. In this case, the current passes through the material with the highest melting point, using resistance heat to increase stirring in the hard material [226].

The EaFSW tool can be categorised into four groups based on the current connection to the FSW tool. The first group involves a hollow FSW tool with a conductive core or coil, as depicted in Fig. 23-a. The electrical heat input and current flow are influenced by the material thickness and conductivity [227]. The second type of tool connection, illustrated in Fig. 23-b, is the simplest. In this configuration, the electrical current flows through the tool using conductive strips [228]. This type results in an increase in the

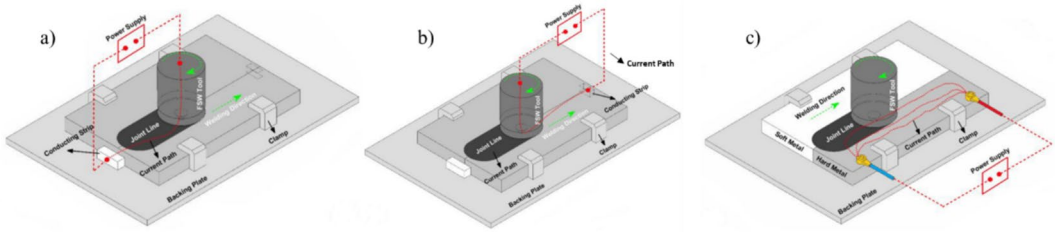

Fig. 22 EaFSW configurations (**a**) heat-treatment, (**b**) preheating, and (**c**) current pass through one workpiece [209]

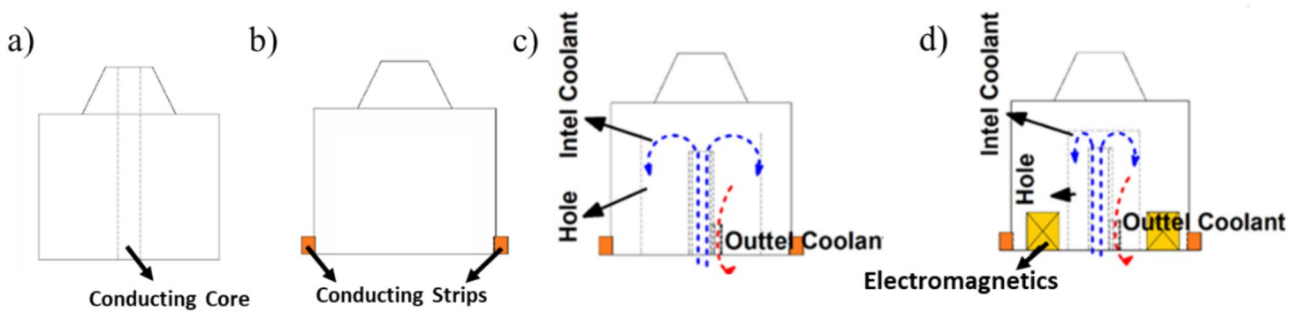

Fig. 23 EaFSW tool categories (**a**) using conductive core, (**b**) using conductive strips, (**c**) using conductive strips and coolant and (**d**) using coolant and electromagnetics [209]

tool temperature, necessitating a cooling system, which is implemented in the third group (Fig. 23-c). The tool in this category is designed with an inside hole to allow a coolant to flow inside it. The coolant can be either a gas (nitrogen or hydrogen) or a liquid (water) [206]. In the fourth type, an electromagnetic or ultrasound vibration system is applied to enhance the quality of the welded joints in either type one or type three [209].

The tool wear in EaFSW and FSW was investigated by Sengupta et al. [229] using a tungsten carbide (WC) tool to join Inconel 601 alloy by preheating the joint type EaFSW. Input parameters included tool speeds and applied current. The findings indicated that tool wear in EaFSW was lower compared to FSW, which was attributed to the developed resistance heat that reduced the load on the tool. Additionally, EaFSW led to a 21.62% increase in UTS. These results align well with those reported in [230]. This paper presents a variant of FSW aiming to minimise or eliminate the root defects that still constitute a major constraint to a wider dissemination of FSW into industrial applications. The concept is based on the use of an external electrical energy source, delivering a high-intensity current, passing through a thin layer of material between the back plate and the lower tip of the tool probe. The heat generated by the Joule effect improves material viscoplasticity in this region, minimising the root defects. The concept was validated by analytical and experimental analysis. Later, a new dedicated tool was designed, manufactured, and tested. Numerical simulations were performed to study the electrical current flow pattern and its effect on the material below the probe tip. The potential use of this variant was shown by reducing the size of the weld root defect, even for significant levels of lack of penetration, without affecting the overall metallurgical characteristics of the welded joints.

Han et al. [225] conducted an investigation into the influence of preheat joint type EaFSW of AZ31B magnesium alloy. Their findings revealed that optimising the current flow and heat input can eliminate the root defect in the joints. As the current increased, the SZ also increased, and the grains exhibited a smoother transition between the SZ and TMAZ. The study demonstrated that the maximum tensile strength was attained by increasing the current up to 200 A. However, the hardness showed only a slight impact from the current variations. These results are consistent with [231] for the same welding type and material and with [232], who utilised an EaFSW tool with a coolant to investigate the effect of electric current on microstructure characteristics and tensile properties of Ti-6Al-4 V alloy welded by EaFSW. A cooling system consisting of water cooling and air cooling was applied to the EaFSW tool to prevent damage caused by high temperatures [233]. The process parameters of 800 rpm for rotational speed, 160 mm/min for traverse speed, and 1.5° tilt angle increased the material flow in welded aluminium alloy. The results showed that the EaFSW process had a positive impact on precipitate distribution in the SZ, thereby improving the joint's overall quality. The study further reported a noteworthy enhancement in UTS and hardness, compared to FSW, with increases of 17.11% and 18.13%, respectively.

Similarly, EaFSW has drawbacks similar to other thermal energy-assisted methods. These include the need for additional preparations, such as cooling and insulation systems, to manage the excessive heat generated by the electrical current. These additional requirements can significantly increase the overall process expenses. To minimize these drawbacks and fully leverage the benefits of EaFSW, further enhancements in process design are necessary. A crucial aspect that requires careful consideration is the thermal history during the welding process, as it plays a vital role in determining the final quality and properties of the weld.

3.4 Arc-assisted FSW

Arc welding is a type of fusion welding that relies on a thermal source to join materials by generating heat through an electric arc. In this process, an electrode connected to a power supply is brought close to the workpiece, creating an electric arc as the current jumps through the air gap. Intense heat from this arc melts the metal at the welding point, fusing the materials together. The electrodes used in arc welding can be either consumable, where they melt and become part of the weld, or non-consumable, like tungsten, which does not melt but still generates the arc necessary for welding [82].

Arc-assisted Friction Stir Welding (AaFSW) operates on a different principle than EaFSW. In EaFSW, the heating source is based on resistance heating, where current passes directly through the workpiece. In contrast, AaFSW maintains an air gap between the electrode and the workpiece, allowing current to pass through and create an arc that generates temperatures high enough to melt the metal [206], as shown in Fig. 24. AaFSW was pioneered by Sindo Kou and Guoping Cao of the Wisconsin Alumni Research Foundation [234]. This technique integrates FSW with arc welding processes like Plasma Arc Welding (PAW) or Gas Tungsten Arc Welding (GTAW) to preheat the material before the FSW tool stirs it. AaFSW is particularly effective for welding high melting point materials, as the heat from arc welding can reach 6,000–8,000 °C with GTAW [235] and 10,000–20,000 °C for the PAW [236]. This temperature enhances the fluidity and plastic flow of the material being welded, making the process more efficient. However, this technique is not without its drawbacks. The integration of arc welding equipment introduces increased complexity and higher energy consumption, which can elevate operational costs. Additionally, the intense heat can also lead to

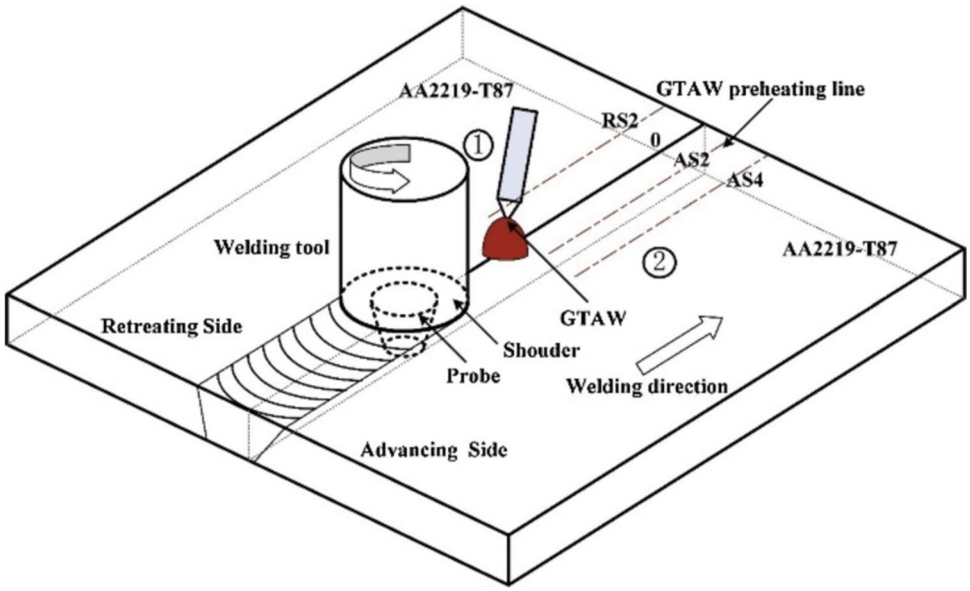

Fig. 24 GTA-assisted FSW process [237]

challenges such as oxide formation and fume generation, which must be managed to ensure the quality of the weld [82]. These challenges may limit the effectiveness and applicability of AaFSW, particularly in scenarios requiring precise control overheat and material properties.

Li et al. [237] applied GTAW as a preheating system in AaFSW of AA2219-T87. They investigated GTAW offsets at four locations on the advancing and retreating sides. The findings showed that preheating at the advancing side enhanced material fluidity and increased the tensile strength of the welded joint by 12.3% while reducing the differences in hardness between the advancing and retreating sides. Additionally, the texture strength in AaFSW was found to be lower than that of FSW, indicating that dynamic recrystallisation was adequately achieved with preheating at the advancing side. Another investigation utilising GTAW as a preheating method was conducted by Yi et al. [238] for welding AA2519-T87 aluminium alloy. Their findings echoed previous results, indicating that AaFSW improved the material flow. Additionally, they observed that the tensile strength and elongation in AaFSW surpassed those achieved in FSW by 16.9% and 209.1%, respectively. Pankaj et al. [239] conducted experimental and numerical analyses of a dissimilar welded joint between DH36 steel and AISI 1008 steel using AaFSW, with PAW as the preheating process. The study observed reduced vertical force, leading to improved weld quality as material flow was enhanced. Various welding parameters, including traverse speed, rotational speed, plasma offset, and preheating current, were investigated to understand their impact on thermal history. A comparative study between FSW and AaFSW revealed that the AaFSW process resulted in reduced grain size, while hardness and impact toughness values were higher compared to those of FSW. These findings align with the results of [240], who conducted a numerical analysis and experimental investigation of AaFSW using AISI 1018 low-carbon steel plates. The study investigated tool welding speeds, the gap between the plasma source and the tool shoulder, and plasma radius as input parameters on comparative thermal history.

Overall, thermally assisted FSW processes offer substantial improvements in process variables, efficiency, and mechanical properties, leading to finer grain structures, enhanced tensile properties, and better microstructural characteristics. However, these methods also introduce several challenges. The increased heat input can cause degradation of mechanical properties, expansion of the HAZ, and growth of brittle precipitate phases, which may compromise joint integrity. Additionally, each thermal energy source has its limitations: induction heating often suffers from uneven heat distribution, laser reflections can lead to reduced energy efficiency and electric and arc heating methods are constrained to conductive materials. Given these issues, there is a pressing need for the development of a cost-effective, high-efficiency secondary energy source that can assist in material softening for FSW. Mechanical energy emerges as a promising alternative, with the potential to address the limitations of current thermal methods and enhance both weld quality and process efficiency. This approach is explored in greater detail in the following section.

3.5 Ultrasonic vibration assisted FSW

Ultrasonic vibration welding is classified as a solid-state welding technique, where no melting occurs during the joining process. Instead, it leverages high-frequency ultrasonic vibrations to weld materials. The underlying principle of this

method involves using mechanical vibrations to stimulate dislocations that have hardened due to deformation, thereby reducing stresses and facilitating further plastic deformation [241]. Notably, the ultrasonic energy required to soften materials is significantly lower than the thermal energy needed, as ultrasonic energy is preferentially absorbed at dislocation sites within the grains, rather than uniformly throughout the material as with thermal energy [206, 241].

Based on these advantages, ultrasonic vibration welding has gained significant attention and is applied not only in ultrasonic welding and brazing but also as an auxiliary technique in FSW. Unlike other hybrid FSW methods that rely on high heat inputs, ultrasonic vibration-assisted friction stir welding (UVaFSW) introduces a novel approach by integrating ultrasonic vibrations to enhance the FSW process without excessive heat. The ultrasonic vibration frequency source softens the material and enhances plastic deformation [242, 243]. UVaFSW can produce defect-free joints with a smooth transition boundary region in the microstructure. Additionally, UVaFSW reduces tool wear, decreases axial forces, increases tool life, and enhances the mechanical properties of welded joints [244].

The ultrasonic vibration system in UVaFSW comprises a generator that produces high-frequency vibrations, which are converted into mechanical oscillations by a transducer. These oscillations are then transmitted through the welding system via a sonotrode or ultrasonic horn. The design of the horn is crucial, as its resonance frequency must match the working frequency of the ultrasonic generator to ensure optimal performance. The efficiency of ultrasonic energy transmission through the horn increases as the contact area between the horn and the weld zone decreases [206].

The ultrasonic horn in UVaFSW can be configured in two primary ways: mounted either directly on the tool (axially or radially) or on the workpiece [245, 246]. Some studies have explored transmitting vibrations from the horn via the backing plate to the workpiece, although this approach is less common [206]. Figure 25 illustrates the various configurations of UVaFSW.

In the configuration shown in Fig. 25-a), the ultrasonic energy is transferred to the welding zone via multiple pathways—from the horn to the tool and then to the material. This setup initially encountered issues with energy loss and tool wear due to the bearing system between the horn and the

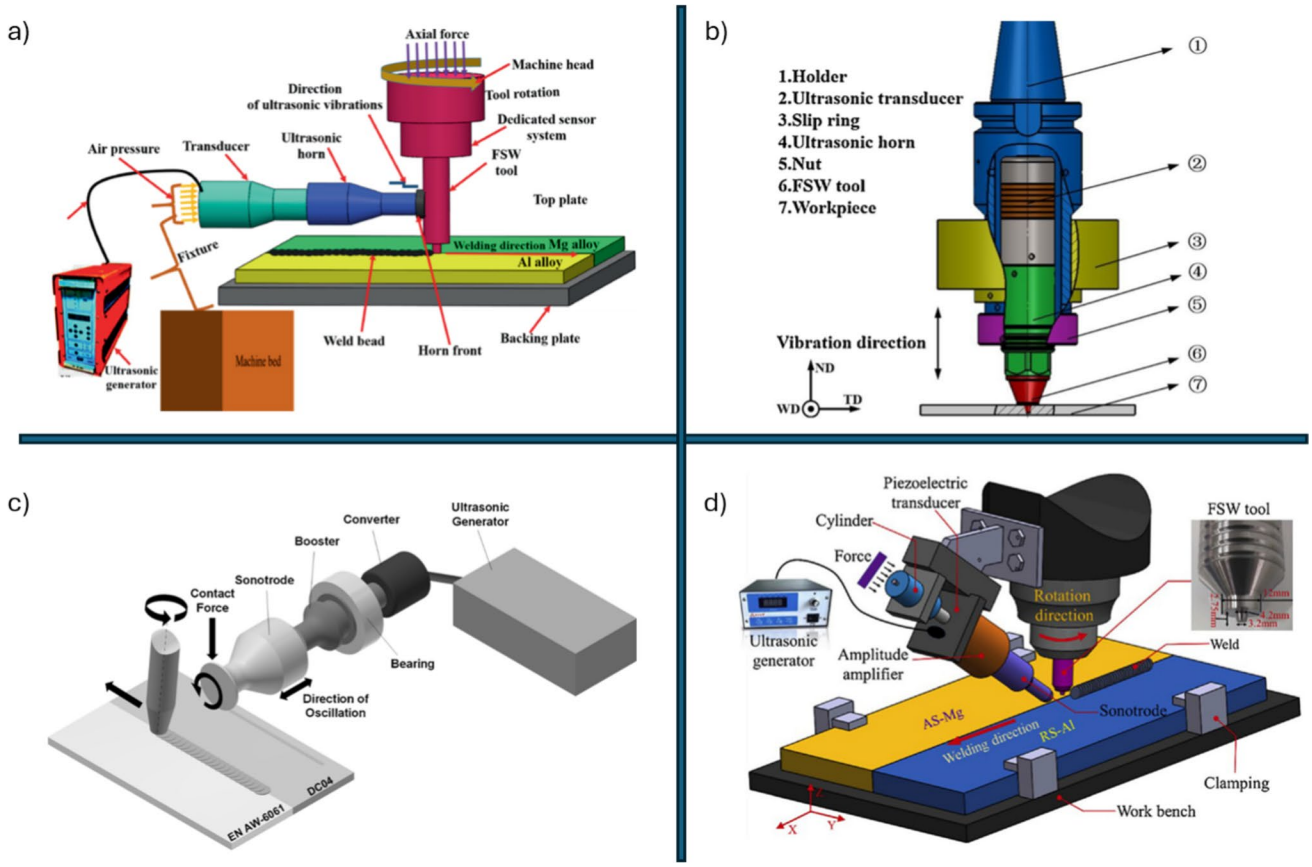

Fig. 25 Various configurations of ultrasonic energy transmission in the UVaFSW process: **a** transmission directly through the tool side [250], (**b**) axial transmission through the tool [252], (**c**) transmission applied to one of the workpieces [254], and (**d**) direct transmission into the weld zone [257]

FSW tool. Researchers in [247, 248] have since improved this configuration by incorporating a roller bearing with the ultrasonic horn, positioning the horn perpendicular to the FSW tool to ensure effective transmission of ultrasonic vibrations into the stir SZ along the welding direction. Further details on this technique are provided in [249, 250].

Another advancement in enhancing ultrasonic vibration transmission into the SZ is shown in Fig. 25-b). This technique, utilized by Ruilin et al. [251], involves applying ultrasonic vibrations axially through the FSW tool. Zhang et al. [252] further investigated this configuration, analysing its impact on the axial force, weld formation, and plastic flow behaviour in UVaFSW compared to conventional FSW of 7N01-T4 aluminium alloy. However, transmitting vibrations through the tool could potentially alter the tool's physical properties due to acoustic effects.

Two additional developments focus on applying ultrasonic vibrations directly to the workpiece. One approach involves placing the horn on the workpieces, as explored in [253]. Thomä et. al [254] implemented a similar setup using an oscillating roll seam module that moves parallel to the FSW tool, as illustrated in Fig. 25-c). Despite its innovation, this configuration suffers from significant energy loss, as the horn is positioned far from the welding zone. Another approach, developed by Liu et al. [255, 256] involves applying the horn at a 45° angle directly on the welding line, with the horn moving in sync with the FSW tool along the weld line, as shown in Fig. 25-d). This method appears to be the most efficient for transmitting ultrasonic energy, as it delivers energy directly into the weld zone. Further investigations into this configuration can be found in [257, 258].

This overview highlights the evolution of ultrasonic vibration integration in FSW, emphasizing various configurations and their associated advantages and challenges. One notable study by Meng et al. [259] evaluated the efficiency of the UVaFSW process to weld dissimilar materials AA6061-T6 and AZ31B Mg alloy. Experimental and numerical studies were conducted. The ultrasonic transducer was applied at the Mg workpiece on the advancing side. They found that the material flow was enhanced due to the vibration, enhancing the weldability of Al/Mg alloys and forming a sound joint with a complex mixture of Al/Mg alloys in the stir zone. The ultrasonic could broaden the process window and then improve tensile properties. They concluded that the ultrasonic vibration could disperse and distribute the smashed IMCs in the SZ and improve tensile properties. Also, the material adhesion problem on the pin was solved due to vibration. Another study was carried out by [244] to weld dissimilar Al/Mg alloys using FSW and UVaFSW. A frequency of 20 kHz with a maximum amplitude of 25 µm (without a load) was applied to weld AA7075-T6 and AZ31B alloys. The ultrasonic effect reduced the thickness of intermetallic compounds (IMCs) and enhanced grain recrystallisation and mechanical properties of the welded joints. Additionally, ultrasonic vibration reduced residual stress, enhancing the stress interaction at the Al/Mg interface associated with thinner IMCs. These findings are in line with studies of dissimilar materials such as Al/Cu [260, 261], Al/Mg [250, 257, 262, 263], Al/Steel [254] and similar materials [252, 264, 265].

However, UVaFSW encounters several challenges, particularly when applied to materials with low ductility or high melting points. These materials can pose difficulties for effective ultrasonic vibration transmission and may not respond well to the vibration-induced softening effects. Moreover, the high-frequency ultrasonic vibrations, although generally beyond the range of human hearing, generate high-pitched noise that can be uncomfortable or potentially harmful to operators. Addressing these issues involves not only refining the ultrasonic vibration parameters but also making advancements in the design of the ultrasonic setup to reduce energy losses during the welding process. Enhanced noise mitigation strategies and improved energy efficiency are essential to maximizing the effectiveness and safety of UVaFSW, ensuring that it can be applied to a broader range of materials and welding scenarios.

Overall, hybrid FSW processes have shown promise in improving defect elimination, mechanical properties, and surface quality for a variety of materials. They typically lead to finer grains, increased hardness, and reduced intermetallic compound thickness. However, there are ongoing challenges, such as controlling current flow in IaFSW, addressing cost and efficiency issues in LaFSW, and reducing tool wear in EaFSW. Further research is needed to assess their long-term performance and effectiveness across diverse materials and conditions. Furthermore, numerical modelling should accompany experimental work better to understand the interactions between external energy sources and materials. Additionally, exploring the combination of multiple techniques could offer further improvements in welding processes.

4 Current status of FSTs

Advancements in FSTs focus on optimizing process parameters and heat treatment to improve joint quality and mechanical properties. Fine-tuning process parameters can yield joint efficiencies up to 98% in dissimilar aluminium alloys [85]. Pre- and post-processing heat treatments play a crucial role in enhancing microstructure, with tailored treatments improving tensile strength and corrosion resistance [102–106].

The ongoing research focuses on evolving the FSP techniques with the incorporation of cooling systems and hybrid FSP, which have significantly improved microstructural

refinement and enhanced material properties [160, 162, 163]. Furthermore, friction stir techniques are being integrated into additive manufacturing, enabling the fabrication of large structures with superior mechanical properties. These methods extend to AFSD, presenting an innovative solution for reusing metal chips as deposition materials [192, 199].

In hybrid FSW, external heat sources significantly improve efficiency and mechanical properties but pose risks such as overheating, which can lead to melting, liquefied cracks, and enlarged heat-affected zones. Effective heat management, including cooling and insulation systems, is critical, particularly when welding materials with different melting points. Research continues to optimize these techniques, including their application to thermoplastic composites, which present unique challenges due to the different behaviours of metals and polymers during welding.

4.1 Summary

FSTs have exhibited significant potential for enhancing microstructures through grain refinement and improving mechanical properties such as hardness, UTS, and YS across a wide range of alloys and composites. This capability positions FSTs as promising solutions for various engineering applications in aerospace, transportation, automotive, marine, and machinery components.

This review provides an overview of the latest developments and rapidly expanding knowledge in FSTs, covering their applications, advantages, inherent challenges, control strategies, and future research directions. The following conclusions can be drawn:

1. Components processed using FSTs exhibit enhanced characteristics across various applications.
2. Notably, the aluminium alloys, known for their high strength-to-weight ratio, demonstrate enhanced properties across various applications when processed using FSTs.
3. In addition to improved mechanical properties, FSTs enhance the corrosion resistance of processed alloys, including aluminium, magnesium, copper, nickel, and titanium.
4. FSTs also play a vital role in minimising the thickness of intermetallic compounds between dissimilar materials, thereby enhancing joint properties. This capability expands the scope of their applications in manufacturing processes.
5. The parameters of FSTs, including tool geometry, rotational and traverse speeds, axial force and cooling conditions, play a crucial role in controlling heat generation and refining microstructures.
6. The FSW process offers numerous advantages over traditional fusion techniques; however, it still requires further development to enhance flexibility compared to conventional welding methods.
7. FSSW and RFSSW demonstrate effectiveness in joining thin materials with improved joint efficiency.
8. FSP enhances mechanical properties through phase transformations and grain refinement in high-strength alloys.
9. Additive friction-based manufacturing techniques (such as FSAM and AFSD) excel in repairing structural defects and improving mechanical properties in comparison with other fusion repairing techniques. However, these techniques face limitations in flexibility and manufacturing accuracy.
10. Temperature distribution in AFSD influences heat generation and deformation mechanisms, which impact mechanical properties. Different deposition materials are characterised by dynamic recrystallisation accompanied by grain growth, precipitate evolution, phase transition, etc. Further research is needed to develop unified constitutive models under transient thermo-mechanical conditions.
11. Hybrid FSW processes reduce axial force, eliminate welding defects in dissimilar materials, and improve mechanical properties and surface morphology.
12. Grain refinement and enhanced hardness are observed in most hybrid FSW processes, along with reduced intermetallic compound (IMC) thickness at material interfaces, leading to improved mechanical properties, particularly in UVaFSW.
13. Challenges remain in hybrid FSW processes, including controlling current flow in IaFSW, addressing efficiency and cost concerns in LaFSW, and designing tools to prevent wear in EaFSW.

Finally, we need to explore hybrid FSTs that combine FSW/FSP with external energy sources like laser heating, ultrasonic vibration, or induction heating. These hybrid methods give you more ways to control the amount of heat that goes into the joint, make it easier for materials to mix at the joint interface, and improve the bonding between different types of metals. This leads to better weld quality and better mechanical properties.

4.2 Future research directions

Despite advancements in friction-based techniques, several challenges must be addressed before these methods can achieve widespread industrial adoption. Future research should focus on:

1. Expanding research on integrating auxiliary techniques such as arc, laser, or ultrasonic methods with FSP and investigating their impact on process efficiency and quality of the process as done for hybrid FSW.
2. Investigating key parameters, such as the cooling effect in hybrid FSTs, which is crucial for achieving ultrafine-grained microstructures in alloys.
3. Establishing a comprehensive database of FSTs and hybrid FST defects, including their shapes, sizes, and corresponding repair techniques. This repository, based on experimental data and numerical simulations, will enhance troubleshooting and process reliability.
4. Developing a defect image database to train AI models for closed-loop control systems. Implementing high-speed optical imaging and correlation techniques based on AI model to enable real-time, in-situ monitoring of defects and mechanical properties.
5. Conducting a Lifecycle Assessment for hybrid FSTs can help evaluate their environmental impact and identify opportunities for reducing such effects through alternative approaches. This assessment will provide valuable insights into the sustainability of FST processes and guide efforts towards minimising their environmental footprint.
6. Although some literature addresses numerical modelling and analysis of LaFSW and EaFSW, comprehensive exploration is needed for numerical simulations of various hybrid FSW techniques. Understanding the underlying mechanism and the relationship of external energy interaction with material flow is crucial. Additionally, a thorough investigation into the microstructural aspects of joints prepared by hybrid FSW is essential to assess the process feasibility for broader applications.
7. Investigate the potential of electrical current to enhance friction stir spot welding. Research should focus on understanding the mechanism of current selection and its effects on weld quality and efficiency.
8. Explore the hybridization of more than two techniques to discover new possibilities and optimize welding processes further. This research could lead to breakthroughs in welding technology, offering enhanced performance and broader application potential.

Acknowledgements The authors appreciate the management of the Department of Mechanical and Construction Engineering, Northumbria University, Newcastle upon Tyne, United Kingdom, for providing funding, workspace, and research facilities for this research.

Funding The authors did not receive any specific grant from funding agencies for the submitted work.

Conflicts of interest The authors declare that they have no conflicts of interest regarding the publication of this paper.

References

1. Ma Z, Feng A, Chen D, Shen J (2018) Recent advances in friction stir welding/processing of aluminum alloys: microstructural evolution and mechanical properties. Crit Rev Solid State Mater Sci 43:269–333
2. Dursun T, Soutis C (2014) Recent developments in advanced aircraft aluminium alloys. Mater Des 1980–2015(56):862–871. https://doi.org/10.1016/j.matdes.2013.12.002
3. Polmear I, StJohn D, Nie J-F, Qian M (2017) Light alloys: metallurgy of the light metals. Butterworth-Heinemann
4. Singh K, Singh G, Singh H (2018) Review on friction stir welding of magnesium alloys. J Magnes Alloy 6:399–416
5. Wei J, He C, Qie M, Li Y, Zhao Y, Qin G, Zuo L (2022) Microstructure refinement and mechanical properties enhancement of wire-arc additive manufactured 2219 aluminum alloy assisted by interlayer friction stir processing. Vacuum 203:111264
6. Zhang C, Huang G, Cao Y, Zhu Y, Huang X, Zhou Y, Li Q, Zeng Q, Liu Q (2020) Microstructure evolution of thermo-mechanically affected zone in dissimilar AA2024/7075 joint produced by friction stir welding. Vacuum 179:109515
7. Gangwar K, Ramulu M (2018) Friction stir welding of titanium alloys: A review. Mater Des 141:230–255
8. Shen Z, Ding Y, Gerlich AP (2020) Advances in friction stir spot welding. Crit Rev Solid State Mater Sci 45:457–534
9. Srivastava M, Rathee S, Maheshwari S, Noor Siddiquee A, Kundra T (2019) A review on recent progress in solid state friction based metal additive manufacturing: friction stir additive techniques. Crit Rev Solid State Mater Sci 44:345–377
10. Rathee S, Maheshwari S, Siddiquee AN, Srivastava M (2018) A review of recent progress in solid state fabrication of composites and functionally graded systems via friction stir processing. Crit Rev Solid State Mater Sci 43:334–366
11. Mehta K (2017) Advanced joining and welding techniques: an overview. In: Gupta K (ed) Advanced manufacturing technologies. Materials forming, machining and tribology. Springer, Cham. https://doi.org/10.1007/978-3-319-56099-1_5
12. Mehta KP, Vilaça P (2022) A review on friction stir-based channeling. Crit Rev Solid State Mater Sci 47:1–45
13. Prabhakar DAP, Shettigar AK, Herbert MA, Patel GCM, Pimenov DY, Giasin K, Prakash C (2022) A comprehensive review of friction stir techniques in structural materials and alloys: challenges and trends. J Market Res 20:3025–3060. https://doi.org/10.1016/j.jmrt.2022.08.034
14. Taheri H, Kilpatrick M, Norvalls M, Harper WJ, Koester LW, Bigelow T, Bond LJ (2019) Investigation of Nondestructive Testing Methods for Friction Stir Welding. Metals 9:624. https://doi.org/10.3390/met9060624
15. Gupta MK (2020) Friction stir process: a green fabrication technique for surface composites—a review paper. SN Appl Sci 2:1–14

16. Dong H, Li X, Xu K, Zang Z, Liu X, Zhang Z, Xiao W, Li Y (2022) A Review on Solid-State-Based Additive Friction Stir Deposition. Aerospace 9:565
17. Vilaça P, Hänninen H, Saukkonen T, Miranda RM (2014) Differences between secondary and primary flash formation on coating of HSS with AISI 316 using friction surfacing. Weld World 58:661–671
18. Padhy GK, Wu CS, Gao S (2018) Friction stir based welding and processing technologies - processes, parameters, microstructures and applications: A review. J Mater Sci Technol 34:1–38. https://doi.org/10.1016/j.jmst.2017.11.029
19. Rajak DK, Pagar DD, Menezes PL, Eyvazian A (2020) Friction-based welding processes: friction welding and friction stir welding. J Adhes Sci Technol 34:2613–2637
20. Heidarzadeh A, Mironov S, Kaibyshev R, Çam G, Simar A, Gerlich A, Khodabakhshi F, Mostafaei A, Field DP, Robson JD (2021) Friction stir welding/processing of metals and alloys: A comprehensive review on microstructural evolution. Prog Mater Sci 117:100752
21. Threadgill PL, Leonard AJ, Shercliff HR, Withers PJ (2009) Friction stir welding of aluminium alloys. Int Mater Rev 54:49–93. https://doi.org/10.1179/174328009X411136
22. Salih OS, Ou H, Sun W, McCartney DG (2015) A review of friction stir welding of aluminium matrix composites. Mater Des 86:61–71. https://doi.org/10.1016/j.matdes.2015.07.071
23. Leon JS, Bharathiraja G, Jayakumar V (2020) A review on friction stir welding in aluminium alloys. In: IOP conference series: materials science and engineering (vol 954, No 1, p 012007). IOP Publishing. https://doi.org/10.1088/1757-899X/954/1/012007
24. Thankachan T, Prakash KS, Kavimani V (2019) Investigating the effects of hybrid reinforcement particles on the microstructural, mechanical and tribological properties of friction stir processed copper surface composites. Compos B Eng 174:107057
25. Kurabayashi K, Tokita S, Sato YS (2022) Effect of Ni addition on the interfacial strength of Al/Cu dissimilar welds produced by friction stir lap welding. Metals 12:453
26. Ebrahimi M, Par M (2019) Twenty-year uninterrupted endeavor of friction stir processing by focusing on copper and its alloys. J Alloy Compd 781:1074–1090
27. Mehta KP, Badheka VJ (2016) A review on dissimilar friction stir welding of copper to aluminum: process, properties, and variants. Mater Manuf Processes 31:233–254
28. Du S, Liu H, Gao Y, Hu Y, Zhou L (2022) Effects of process parameters on joint formation and tool wear behavior in friction stir welded TA5 alloy. Int J Adv Manuf Technol 123:2531–2547
29. Chumaevskii A, Amirov A, Ivanov A, Rubtsov V, Kolubaev E (2023) Friction Stir Welding/Processing of Various Metals with Working Tools of Different Materials and Its Peculiarities for Titanium Alloys: A Review. Metals 13:970
30. Zhang W, Ding H, Cai M, Yang W, Li J (2019) Low-temperature superplastic deformation mechanism in Ti–6Al–4V alloy processed by friction stir processing. Mater Sci Eng A 764:138261
31. Tarasov S, Amirov A, Chumaevskiy A, Savchenko N, Rubtsov VE, Ivanov A, Moskvichev E, Kolubaev E (2022) Friction Stir Welding of Ti-6Al-4V Using a Liquid-Cooled Nickel Superalloy Tool. Technologies 10:118
32. Vysotskiy I, Zhemchuzhnikova D, Malopheyev S, Mironov S, Kaibyshev R (2020) Microstructure evolution and strengthening mechanisms in friction-stir welded Al–Mg–Sc alloy. Mater Sci Eng A 770:138540
33. Kalashnikova T, Knyazhev E, Gurianov D, Chumaevskii A, Vorontsov A, Kalashnikov K, Teryukalova N, Kolubaev E (2022) Structure, Mechanical Properties and Friction Characteristics of the Al-Mg-Sc Alloy Modified by Friction Stir Processing with the Mo Powder Addition. Metals 12:1015
34. Kalashnikova T, Chumaevskii A, Kalashnikov K, Fortuna S, Kolubaev E, Tarasov S (2020) Microstructural analysis of friction stir butt welded Al-Mg-Sc-Zr alloy heavy gauge sheets. Metals 10:806
35. Sun Y, Chen X, Xie J, Wang C, An Y, Liu Q (2022) High strain rate superplasticity and secondary strain hardening of Al-Mg-Sc-Zr alloy produced by friction stir processing. Mater Today Commun 33:104217
36. Mohan DG, Wu C (2021) A review on friction stir welding of steels. Chin J Mech Eng 34:1–29
37. Karami V, Dariani BM, Hashemi R (2021) Investigation of forming limit curves and mechanical properties of 316 stainless steel/St37 steel tailor-welded blanks produced by tungsten inert gas and friction stir welding method. CIRP J Manuf Sci Technol 32:437–446
38. Mohan DG, Gopi S (2021) Influence of In-situ induction heated friction stir welding on tensile, microhardness, corrosion resistance and microstructural properties of martensitic steel. Eng Res Exp 3:025023
39. Cui L, Zhang C, Liu Y-c, Liu X-g, Wang D-p, Li H-j (2018) Recent progress in friction stir welding tools used for steels. J Iron Steel Res Int 25:477–486
40. Mohan DG, Gopi S, Rajasekar V (2018) Effect of induction heated friction stir welding on corrosive behaviour, mechanical properties and microstructure of AISI 410 stainless steel. Indian J Eng Mater Sci 25:203–208
41. Isa MSM, Moghadasi K, Ariffin MA, Raja S, bin Muhamad MR, Yusof F, Jamaludin MF, bin Yusoff N, bin Ab Karim MS (2021) Recent research progress in friction stir welding of aluminium and copper dissimilar joint: a review. J Mater Res Technol 15:2735–2780
42. He F, Wu C, Shi L (2023) Phase-field simulation of dynamic recrystallization in friction stir weld nugget zone of dissimilar Al/Mg alloys. J Mater Res Technol 27:2670–2683. https://doi.org/10.1016/j.jmrt.2023.10.115
43. Gadakh VS, Badheka VJ, Mulay AS (2021) Solid-state joining of aluminum to titanium: a review. Proc Inst Mech Eng Part L: J Mater: Des Appl 235:1757–1799
44. Deng H, Chen Y, Jia Y, Pang Y, Zhang T, Wang S, Yin L (2021) Microstructure and mechanical properties of dissimilar NiTi/Ti6Al4V joints via back-heating assisted friction stir welding. J Manuf Process 64:379–391
45. Huang T, Zhang Z, Liu J, Chen S, Xie Y, Meng X, Huang Y, Wan L (2022) Interface formation of Medium-thick AA6061 Al/AZ31B Mg dissimilar submerged friction stir welding joints. Materials 15:5520
46. Zhou L, Zhang R, Li G, Zhou W, Huang Y, Song X (2018) Effect of pin profile on microstructure and mechanical properties of friction stir spot welded Al-Cu dissimilar metals. J Manuf Process 36:1–9
47. Shankar S, Vilaça P, Dash P, Chattopadhyaya S, Hloch S (2019) Joint strength evaluation of friction stir welded Al-Cu dissimilar alloys. Measurement 146:892–902
48. Khojastehnezhad VM, Pourasl HH (2018) Microstructural characterization and mechanical properties of aluminum 6061–T6 plates welded with copper insert plate (Al/Cu/Al) using friction stir welding. Trans Nonferrous Met Soc China 28:415–426
49. Snyder B, Strauss AM (2021) In-process cooling of friction stir extruded joints for increased weld performance via compressed air, water, granulated dry ice, and liquid nitrogen. J Manuf Process 68:1004–1017
50. Xu N, Qiu Z-h, Ren Z-k, Shen J, Wang D, Song Q-n, Zhao J-h, Jiang Y-f, Bao Y-f (2023) Enhanced strength and ductility of

rapid cooling friction stir welded ultralight Mg–14Li–1Al alloy joint. J Market Res 23:4444–4453
51. Nazari M, Eskandari H, Khodabakhshi F (2019) Production and characterization of an advanced AA6061-Graphene-TiB2 hybrid surface nanocomposite by multi-pass friction stir processing. Surf Coat Technol 377:124914
52. Abraham SJ, Dinaharan I, Selvam JDR, Akinlabi ET (2019) Microstructural characterization of vanadium particles reinforced AA6063 aluminum matrix composites via friction stir processing with improved tensile strength and appreciable ductility. Compos Commun 12:54–58
53. Bourkhani RD, Eivani A, Nateghi H (2019) Through-thickness inhomogeneity in microstructure and tensile properties and tribological performance of friction stir processed AA1050-Al2O3 nanocomposite. Compos B Eng 174:107061
54. Dinaharan I, Akinlabi ET (2018) Low cost metal matrix composites based on aluminum, magnesium and copper reinforced with fly ash prepared using friction stir processing. Compos Commun 9:22–26
55. Muhammad NA, Wu C, Tian W (2019) Effect of ultrasonic vibration on the intermetallic compound layer formation in Al/Cu friction stir weld joints. J Alloy Compd 785:512–522
56. Yaduwanshi DK, Bag S, Pal S (2015) Hybrid friction stir welding of similar and dissimilar materials. In: Narayanan RG, Dixit US (eds) Advances in material forming and joining. Springer India, New Delhi, pp 323–349
57. Anand R, Sridhar V (2020) Studies on process parameters and tool geometry selecting aspects of friction stir welding–A review. Mater Today: Proc 27:576–583
58. Zhong YB, Wu CS, Padhy GK (2017) Effect of ultrasonic vibration on welding load, temperature and material flow in friction stir welding. J Mater Process Technol 239:273–283. https://doi.org/10.1016/j.jmatprotec.2016.08.025
59. Ambrosio D, Morisada Y, Ushioda K, Fujii H (2023) Material flow in friction stir welding: a review. J Mater Process Technol 320:118116. https://doi.org/10.1016/j.jmatprotec.2023.118116
60. Amatullah M, Jan M, Farooq M, Zargar AS, Maqbool A, Khan NZ (2022) Effect of tool rotational speed on the friction stir welded aluminum alloys: A review. Mater Today: Proc 62:245–250
61. Ethiraj N, Sivabalan T, Sivakumar B, Vignesh Amar S, Vengadeswaran N, Vetrivel K (2020) Effect of tool rotational speed on the tensile and microstructural properties of friction stir welded different grades of stainless steel joints. Int J Eng 33:141–147
62. Machniewicz T, Nosal P, Korbel A, Hebda M (2020) Effect of FSW traverse speed on mechanical properties of copper plate joints. Materials 13:1937
63. Banjare PN, Manoj MK (2020) Effect of tool RPM and tool travers speed on mechanical properties of friction stir welded joints of dissimilar aluminium alloys. Int J Mech Prod Eng Res Dev 10:215–222
64. Kaushik P, Dwivedi DK (2021) Effect of tool geometry in dissimilar Al-steel friction stir welding. J Manuf Process 68:198–208
65. Vairis A, Petousis M, Mountakis N, Tsarouchidou C, Vidakis N (2022) The Effect of Tool Geometry on the Strength of FSW Aluminum Thin Sheets. Materials 15:8187
66 Yaknesh S, Sampathkumar K, Sevvel P (2022) Effect of tool pin geometry and process parameters during FSW of dissimilar alloys of Mg. Mater Res 25:e20210508
67. Memon S, Fydrych D, Fernandez AC, Derazkola HA, Derazkola HA (2021) Effects of FSW tool plunge depth on properties of an Al-Mg-Si alloy T-joint: Thermomechanical modeling and experimental evaluation. Materials 14:4754
68. Thakur A, Sharma V, Bhadauria SS (2021) Effect of tool tilt angle on weld joint strength and microstructural characterization of double-sided friction stir welding of AZ31B magnesium alloy. CIRP J Manuf Sci Technol 35:132–145
69. Lambiase F, Grossi V, Paoletti A (2020) Effect of tilt angle in FSW of polycarbonate sheets in butt configuration. Int J Adv Manuf Technol 107:489–501
70 Elsheikh AH (2023) Applications of machine learning in friction stir welding: Prediction of joint properties, real-time control and tool failure diagnosis. Eng Appl Artif Intell 121:105961. https://doi.org/10.1016/j.engappai.2023.105961
71. Chen P, Zou S, Chen J, Qin S, Yang Q, Zhang Z, Jia Z, Zhang L, Jiang T, Liu Q (2021) Effect of rotation speed on microstructure evolution and mechanical properties of nugget zone in 2195–T8 Al-Li alloy friction stir welding joints. Mater Charact 176:111079
72. Wu B, Ibrahim M, Raja S, Yusof F, Muhamad MRB, Huang R, Zhang Y, Badruddin IA, Hussien M, Kamangar S (2022) The influence of reinforcement particles friction stir processing on microstructure, mechanical properties, tribological and corrosion behaviors: A review. J Mater Res Technol 20:1940–75
73. Geng P, Ma Y, Ma N, Ma H, Aoki Y, Liu H, Fujii H, Chen C (2022) Effects of rotation tool-induced heat and material flow behaviour on friction stir lapped Al/steel joint formation and resultant microstructure. Int J Mach Tools Manuf 174:103858
74. Mahto RP, Kumar R, Pal SK (2020) Characterizations of weld defects, intermetallic compounds and mechanical properties of friction stir lap welded dissimilar alloys. Mater Charact 160:110115
75. Baratzadeh F, Boldsaikhan E, Nair R, Burford D, Lankarani H (2020) Investigation of mechanical properties of AA6082-T6/AA6063-T6 friction stir lap welds. J Adv Join Process 1:100011
76. Chitturi V, Pedapati SR, Awang M (2020) Investigation of weld zone and fracture surface of friction stir lap welded 5052 aluminum alloy and 304 stainless steel joints. Coatings 10:1062
77. Zhao Y, Luo Y, Lu Y, He Y, Guo X, Wang S, Cui H, Zhang Y, Wang Z (2021) Effect of welding parameters on the microstructures and mechanical properties of double-pass aluminum/magnesium dissimilar metal friction stir lap welding joint. Mater Today Commun 26:102132
78. Seleman MME-S, Ahmed MMZ, Ramadan RM, Zaki BA (2022) Effect of FSW Parameters on the Microstructure and Mechanical Properties of T-Joints between Dissimilar Al-Alloys. Int J Integr Eng 14:1–12
79. Su Y, Li W, Gao F, Vairis A (2022) Effect of FSW process on anisotropic of titanium alloy T-joint. Mater Manuf Process 37:25–33
80. Derazkola HA, Kordani N, Derazkola HA (2021) Effects of friction stir welding tool tilt angle on properties of Al-Mg-Si alloy T-joint. CIRP J Manuf Sci Technol 33:264–276
81. Grong O, Sandnes L, Ferro P, Berto F (2021) Hybrid metal extrusion and bonding. Handbook of Welding: Processes. Nova Science Publishers Inc, Control and Simulation, pp 237–291
82. Saha R, Biswas P (2022) Current status and development of external energy-assisted friction stir welding processes: a review. Weld World 66:577–609. https://doi.org/10.1007/s40194-021-01228-7
83. Meng X, Huang Y, Cao J, Shen J, dos Santos JF (2021) Recent progress on control strategies for inherent issues in friction stir welding. Prog Mater Sci 115:100706
84. Avettand-Fènoël M-N, Simar A (2016) A review about friction stir welding of metal matrix composites. Mater Charact 120:1–17
85. Ahmed MM, Ataya S, El-Sayed Seleman MM, Mahdy AM, Alsaleh NA, Ahmed E (2020) Heat input and mechanical properties investigation of friction stir welded aa5083/aa5754 and aa5083/aa7020. Metals 11:68

86. Viscusi A, Astarita A, Prisco U (2019) Mechanical properties optimization of friction stir welded lap joints in aluminium alloy. Adv Mater Sci Eng 2019:3832873
87. Wang Y, Ma H, Chai P, Zhang Y (2021) Strength and fracture behavior of AA2A14-T6 aluminum alloy friction stir welded joints. Weld World 65:1483–1499
88. Zamani SMM, Behdinan K, Razfar MR, Fatmehsari DH, Mohandesi JA (2021) Studying the effects of process parameters on the mechanical properties in friction stir welding of Al-SiC composite sheets. Int J Adv Manuf Technol 113:3629–3641
89. Sun Y, Liu W, Li Y, Gong W, Ju C (2022) The influence of tool shape on plastic metal flow, microstructure and properties of friction stir welded 2024 aluminum alloy joints. Metals 12:408
90. Chandana R, Saraswathamma K (2023) Impact of tool pin profiles in friction stir welding process-A review. Mater Today: Proc 76:602–606
91. Zhang YN, Cao X, Larose S, Wanjara P (2012) Review of tools for friction stir welding and processing. Can Metall Q 51:250–261. https://doi.org/10.1179/1879139512Y.0000000015
92. Wang X, Xiao Y, Shi L, Zhai M, Wu C, Chen G (2023) Revealing the mechanism of tool tilting on suppressing the formation of void defects in friction stir welding. J Mater Res Technol 25:38–54. https://doi.org/10.1016/j.jmrt.2023.05.184
93. Khan AS, Badheka VJ, Chaudhari AB, Gadakh VS (2023) Experimental investigation of friction stir welding of aluminum alloy AA8090-T3 using taguchi method. J Mater Eng Perform 32:4787–4795
94. Rabiezadeh A, Salafzon A, Mostafavi N (2024) Dissimilar welding of AA5083/AA7039 by self-reacting friction stir welding. J Adhes Sci Technol 38:70–91
95. Sahali MA, Aini A, Bouzit L, Himed L, Benaissa B (2023) Experimental modeling and multi-objective optimization of friction stir welding parameters of AA 3004 aluminum alloy. Int J Adv Manuf Technol 124:1229–1244
96. Janeczek A, Tomków J, Fydrych D (2021) The influence of tool shape and process parameters on the mechanical properties of AW-3004 aluminium alloy friction stir welded joints. Materials 14:3244
97. Ahmed MM, Essa AR, Ataya S, El-Sayed Seleman MM, El-Aty AA, Alzahrani B, Touileb K, Bakkar A, Ponnore JJ, Mohamed AY (2023) Friction Stir Welding of AA5754-H24: Impact of Tool Pin Eccentricity and Welding Speed on Grain Structure, Crystallographic Texture, and Mechanical Properties. Materials 16:2031
98. He X, Gu F, Ball A (2014) A review of numerical analysis of friction stir welding. Prog Mater Sci 65:1–66
99. Sharma Y, Mehta A, Vasudev H, Jeyaprakash N, Prashar G, Prakash C (2023) Analysis of friction stir welds using numerical modelling approach: a comprehensive review. Int J Interact Des Manuf 18:5329–5342. https://doi.org/10.1007/s12008-023-01324-6
100. Salih OS, Neate N, Ou H, Sun W (2020) Influence of process parameters on the microstructural evolution and mechanical characterisations of friction stir welded Al-Mg-Si alloy. J Mater Process Technol 275:116366
101. Liu Q, Han R, Gao Y, Ke L (2021) Numerical investigation on thermo-mechanical and material flow characteristics in friction stir welding for aluminum profile joint. Int J Adv Manuf Technol 114:2457–2469
102. Kalinenko A, Mishin V, Shishov I, Malopheyev S, Zuiko I, Novikov V, Mironov S, Kaibyshev R, Semiatin SL (2022) Mechanisms of abnormal grain growth in friction-stir-welded aluminum alloy 6061–T6. Mater Charact 194:112473
103. Khalilabad MM, Zedan Y, Texier D, Jahazi M, Bocher P (2022) Effect of heat treatments on microstructural and mechanical characteristics of dissimilar friction stir welded 2198/2024 aluminum alloys. J Adhes Sci Technol 36:221–239
104. Wang Y, Chen Y, Zhou L, Shao Y, Liu L, Jiang J (2023) Improving the corrosion resistance of friction stir welding joint of 7050 Al alloy via optimizing the process route. J Market Res 24:8098–8108
105. Gupta S, Haridas RS, Agrawal P, Mishra RS, Doherty KJ (2022) Influence of welding parameters on mechanical, microstructure, and corrosion behavior of friction stir welded Al 7017 alloy. Mater Sci Eng, A 846:143303
106. Dong J, Zhang D, Zhang W, Cao G, Qiu C (2023) Effect of post-weld heat treatments on the microstructure and mechanical properties of underwater friction stir welded joints of 7003–T4/6060-T4 aluminium alloys. Mater Sci Eng A 862:144423
107. Li H, Qin W, Liu D, Li Q, Wu Y (2018) Design of friction stir welding tools reducing heat flow into spindle. Int J Adv Manuf Technol 94:1925–1932
108. Leoni F, Grong Ø, Ferro P, Berto F (2020) A semi-analytical model for the heat generation during hybrid metal extrusion and bonding (Hyb). Materials 14:170
109. Tognan A, Sandnes L, Totis G, Sortino M, Berto F, Grong Ø, Salvati E (2022) Evaluation and origin of residual stress in hybrid metal and extrusion bonding and comparison with friction stir welding. Int J Mech Sci 218:107089
110. Sandnes L, Grong Ø, Torgersen J, Welo T, Berto F (2018) Exploring the hybrid metal extrusion and bonding process for butt welding of Al–Mg–Si alloys. Int J Adv Manuf Technol 98:1059–1065
111. Blindheim J, Grong Ø, Welo T, Steinert M (2020) On the mechanical integrity of AA6082 3D structures deposited by hybrid metal extrusion & bonding additive manufacturing. J Mater Process Technol 282:116684
112. Sandnes L, Bergh T, Grong Ø, Holmestad R, Vullum PE, Berto F (2021) Interface microstructure and tensile properties of a third generation aluminium-steel butt weld produced using the Hybrid Metal Extrusion & Bonding (HYB) process. Mater Sci Eng A 809:140975
113. Bergh T, Sandnes L, Johnstone DN, Grong Ø, Berto F, Holmestad R, Midgley PA, Vullum PE (2021) Microstructural and mechanical characterisation of a second generation hybrid metal extrusion & bonding aluminium-steel butt joint. Mater Charact 173:110761
114. Bergh T, Fyhn H, Sandnes L, Blindheim J, Grong Ø, Holmestad R, Berto F, Vullum PE (2023) Multi-material Joining of an Aluminum Alloy to Copper, Steel, and Titanium by Hybrid Metal Extrusion & Bonding. Metall Mater Trans A 54:2689–2702
115. Grong Ø, Sandnes L, Berto F (2019) A status report on the hybrid metal extrusion & bonding (HYB) process and its applications. Mater Des Process Commun 1:e41
116 Sharma C, Tripathi A, Upadhyay V, Verma V, Sharma SK (2021) Friction stir spot welding-process and weld properties: a review. J Inst Eng (India): Ser D 102(2):549–565
117. Suryanarayanan R, Sridhar V (2021) Studies on the influence of process parameters in friction stir spot welded joints–A review. Mater Today: Proc 37:2695–2702
118. Chu Q, Hao S, Li W, Yang X, Zou Y, Wu D (2021) Impact of shoulder morphology on macrostructural forming and the texture development during probeless friction stir spot welding. J Market Res 12:2042–2054
119. Yan Y, Shen Y, Huang G, Hou W, Ni R (2021) Friction stir spot welding of dissimilar ABS and PA6 by a tool with newly designed tooth-shaped flat pin. J Manuf Process 66:521–531
120. Wang Z, Ma G, Yu B, Xue P, Xie G, Zhang H, Ni D, Xiao B, Ma Z (2020) Improving mechanical properties of friction-stir-spot-welded advanced ultra-high-strength steel with additional water cooling. Sci Technol Weld Joining 25:336–344

121. Fu B, Shen J, Suhuddin UF, Chen T, dos Santos JF, Klusemann B, Rethmeier M (2021) Improved mechanical properties of cast Mg alloy welds via texture weakening by differential rotation refill friction stir spot welding. Scripta Mater 203:114113
122. Çam G, Javaheri V, Heidarzadeh A (2023) Advances in FSW and FSSW of dissimilar Al-alloy plates. J Adhes Sci Technol 37:162–194
123. Yang X, Fu T, Li W (2014) Friction Stir Spot Welding: A Review on Joint Macro-and Microstructure, Property, and Process Modelling. Adv Mater Sci Eng 2014:697170
124. Palanivel S, Sidhar H, Mishra R (2015) Friction stir additive manufacturing: route to high structural performance. Jom 67:616–621
125. Zhang Z, Tan Z-J, Li J-Y, Zu Y-F, Sha J-J (2020) Integrated modeling of process–microstructure–property relations in friction stir additive manufacturing. Acta Metall Sin (English Letters) 33:75–87
126. Mishra RS, Haridas RS, Agrawal P (2022) Friction stir-based additive manufacturing. Sci Technol Weld Join 27:141–165. https://doi.org/10.1080/13621718.2022.2027663
127. Lu IK, Reynolds AP (2021) Innovative friction stir additive manufacturing of cast 2050 Al–Cu–Li aluminum alloy. Progress in Additive Manufacturing 6:471–477
128. Zhang Z, Tan Z, Li J, Zu Y, Liu W, Sha J (2019) Experimental and numerical studies of re-stirring and re-heating effects on mechanical properties in friction stir additive manufacturing. Int J Adv Manuf Technol 104:767–784
129. Palanivel S, Nelaturu P, Glass B, Mishra R (2015) Friction stir additive manufacturing for high structural performance through microstructural control in an Mg based WE43 alloy. Mater Des 1980–2015(65):934–952
130. Srivastava AK, Kumar N, Dixit AR (2021) Friction stir additive manufacturing–An innovative tool to enhance mechanical and microstructural properties. Mater Sci Eng B 263:114832
131. Reddy KV, Naik RB, Reddy GM, Chakravarthy P, Janakiram S, Kumar RA (2021) Damping capacity of aluminium surface layers developed through friction stir processing. Mater Lett 298:130031
132. Huang W, Jiang L, Liu C, Chen C, Guo Y, Guo F (2019) The Microstructure Morphology and Texture Evolution of α-Ti in Ti-6Al-4V Alloy During Friction Stir Processing With Low Rotation Speed and Traverse Speed. Adv Eng Mater 21:1900250
133. Tripathi H, Bharti A, Saxena KK, Kumar N (2022) Improvement in mechanical properties of structural AZ91 magnesium alloy processed by friction stir processing. Adv Mater Process Technol 8:1543–1556
134. Orozco-Caballero A, Álvarez-Leal M, Hidalgo-Manrique P, Cepeda-Jiménez CM, Ruano OA, Carreño F (2017) Grain size versus microstructural stability in the high strain rate superplastic response of a severely friction stir processed Al-Zn-Mg-Cu alloy. Mater Sci Eng A 680:329–337
135. Jiang L, Huang W, Liu C, Guo Y, Chen C, Wang J, Yu W (2019) The effects of stored energy on wear resistance of friction stir processed pure Ti. Results Phys 12:1276–1284
136. Bandil K, Vashisth H, Kumar S, Verma L, Jamwal A, Kumar D, Singh N, Sadasivuni KK, Gupta P (2019) Microstructural, mechanical and corrosion behaviour of Al–Si alloy reinforced with SiC metal matrix composite. J Compos Mater 53:4215–4223
137. Su J-Q, Nelson T, Sterling C (2006) Grain refinement of aluminum alloys by friction stir processing. Phil Mag 86:1–24
138. Patel V, Li W, Vairis A, Badheka V (2019) Recent development in friction stir processing as a solid-state grain refinement technique: microstructural evolution and property enhancement. Crit Rev Solid State Mater Sci 44:378–426
139. Khodabakhshi F, Derazkola HA, Gerlich A (2020) Monte Carlo simulation of grain refinement during friction stir processing. J Mater Sci 55:13438–13456
140. Kulekci MK, Esme U, Buldum B (2016) Critical analysis of friction stir-based manufacturing processes. Int J Adv Manuf Technol 85:1687–1712
141. Samanta A, Das H, Grant GJ, Jana S (2022) Effect of tool design and pass strategy on defect elimination and uniform, enhanced tensile properties of friction stir processed high-pressure die-cast A380 alloy. Mater Sci Eng, A 861:144388
142. Kumar RA, Kumar RA, Ahamed KA, Alstyn BD, Vignesh V (2019) Review of friction stir processing of aluminium alloys. Mater Today: Proc 16:1048–1054
143. Gangil N, Siddiquee AN, Maheshwari S (2017) Aluminium based in-situ composite fabrication through friction stir processing: A review. J Alloys Comp 715:91–104. https://doi.org/10.1016/j.jallcom.2017.04.309
144. Kalashnikov K, Chumaevskii A, Kalashnikova T, Cheremnov A, Moskvichev E, Amirov A, Krasnoveikin V, Kolubaev E (2021) Friction Stir Processing of Additively Manufactured Ti-6Al-4V Alloy: Structure Modification and Mechanical Properties. Metals 12:55
145. Zykova A, Vorontsov A, Chumaevskii A, Gurianov D, Gusarova A, Kolubaev E, Tarasov S (2022) Structural evolution of contact parts of the friction stir processing heat-resistant nickel alloy tool used for multi-pass processing of Ti6Al4V/(Cu+ Al) system. Wear 488:204138
146. Zykova A, Vorontsov A, Chumaevskii A, Gurianov D, Savchenko N, Gusarova A, Kolubaev E, Tarasov S (2022) In Situ Intermetallics-Reinforced Composite Prepared Using Multi-Pass Friction Stir Processing of Copper Powder on a Ti6Al4V Alloy. Materials 15:2428
147. Amirov A, Eliseev A, Kolubaev E, Filippov A, Rubtsov V (2020) Wear of ZhS6U nickel superalloy tool in friction stir processing on commercially pure titanium. Metals 10:799
148. Singh AK, Ratrey P, Astarita A, Franchitti S, Mishra A, Arora A (2021) Enhanced cytocompatibility and mechanical properties of electron beam melted Ti-6Al-4V by friction stir processing. J Manuf Process 72:400–410
149. Singh AK, Kaushik L, Singh J, Das H, Mondal M, Hong S-T, Choi S-H (2022) Evolution of microstructure and texture in the stir zone of commercially pure titanium during friction stir processing. Int J Plast 150:103184
150. Patel V, Li W, Andersson J, Li N (2022) Enhancing grain refinement and corrosion behavior in AZ31B magnesium alloy via stationary shoulder friction stir processing. J Mater Res Technol 17:3150–3156
151. Eivani A, Mehdizade M, Chabok S, Zhou J (2021) Applying multi-pass friction stir processing to refine the microstructure and enhance the strength, ductility and corrosion resistance of WE43 magnesium alloy. J Mater Res Technol 12:1946–1957
152. Kalashnikov K, Tarasov SY, Chumaevskii A, Fortuna S, Eliseev A, Ivanov A (2019) Towards aging in a multipass friction stir–processed AA2024. Int J Adv Manuf Technol 103:2121–2132
153. Zykova A, Chumaevskii A, Gusarova A, Gurianov D, Kalashnikova T, Savchenko N, Kolubaev E, Tarasov S (2021) Evolution of microstructure in friction stir processed dissimilar CuZn37/AA5056 stir zone. Materials 14:5208
154. Tarasov SY, Rubtsov V, Fortuna S, Eliseev A, Chumaevsky A, Kalashnikova T, Kolubaev E (2017) Ultrasonic-assisted aging in friction stir welding on Al-Cu-Li-Mg aluminum alloy. Weld World 61:679–690
155. Patel VV, Badheka V, Kumar A (2016) Friction stir processing as a novel technique to achieve superplasticity in aluminum alloys: process variables, variants, and applications. Metallogr Microstruct Anal 5:278–293

156. Mathur V, Patel GCM, Shettigar A (2019) Reinforcement of titanium dioxide nanoparticles in aluminium alloy AA 5052 through friction stir process. Adv Mater Process Technol 5:329–337
157. Vakili-Azghandi M, Roknian M, Szpunar JA, Mousavizade SM (2020) Surface modification of pure titanium via friction stir processing: Microstructure evolution and dry sliding wear performance. J Alloy Compd 816:152557
158. Patel VV, Badheka V, Kumar A (2017) Effect of polygonal pin profiles on friction stir processed superplasticity of AA7075 alloy. J Mater Process Technol 240:68–76. https://doi.org/10.1016/j.jmatprotec.2016.09.009
159. Zhang H, Xue P, Wang D, Wu L, Ni D, Xiao B, Ma Z (2019) A novel approach to achieve high yield strength high nitrogen stainless steel with superior ductility and corrosion resistance. Mater Lett 242:91–94
160. Ralls AM, Daroonparvar M, Kasar AK, Misra M, Menezes PL (2023) Influence of friction stir processing on the friction, wear and corrosion mechanisms of solid-state additively manufactured 316L duplex stainless steel. Tribol Int 178:108033
161. Patel V, Li W, Xu Y (2019) Stationary shoulder tool in friction stir processing: a novel low heat input tooling system for magnesium alloy. Mater Manuf Process 34:177–182
162. He C, Wei J, Li Y, Zhang Z, Tian N, Qin G, Zuo L (2023) Improvement of microstructure and fatigue performance of wire-arc additive manufactured 4043 aluminum alloy assisted by interlayer friction stir processing. J Mater Sci Technol 133:183–194. https://doi.org/10.1016/j.jmst.2022.07.001
163. Bai X, Wang Y, Lv H, Zhang H, Zhou X (2023) Improving Comprehensive Properties of Wire Arc Additively Manufactured Al-4043 Alloy by Bilateral Friction Stir Post-processing. J Mater Eng Perform. https://doi.org/10.1007/s11665-023-09047-1
164. Kalashnikova T, Chumaevskii A, Kalashnikov K, Knyazhev E, Gurianov D, Panfilov A, Nikonov S, Rubtsov V, Kolubaev E (2022) Regularities of Friction Stir Processing Hardening of Aluminum Alloy Products Made by Wire-Feed Electron Beam Additive Manufacturing. Metals 12:183
165. Mabuwa S, Msomi V, Mehdi H, Saxena KK (2023) Effect of material positioning on Si-rich TIG welded joints of AA6082 and AA8011 by friction stir processing. J Adhes Sci Technol 37:2484–2502
166. Sharma DK, Patel V, Badheka V, Mehta K, Upadhyay G (2019) Fabrication of hybrid surface composites AA6061/(B4C+ MoS2) via friction stir processing. J Tribol 141:052201
167. Barati M, Abbasi M, Abedini M (2019) The effects of friction stir processing and friction stir vibration processing on mechanical, wear and corrosion characteristics of Al6061/SiO2 surface composite. J Manuf Process 45:491–497. https://doi.org/10.1016/j.jmapro.2019.07.034
168. Prabhu MS, Perumal AE, Arulvel S, Issac RF (2019) Friction and wear measurements of friction stir processed aluminium alloy 6082/CaCO3 composite. Measurement 142:10–20
169. Deore H, Mishra J, Rao A, Mehtani H, Hiwarkar V (2019) Effect of filler material and post process ageing treatment on microstructure, mechanical properties and wear behaviour of friction stir processed AA 7075 surface composites. Surf Coat Technol 374:52–64
170. Kumar TS, Priyadharshini GS, Shalini S, Kumar KK, Subramanian R (2019) Characterization of NbC-reinforced AA7075 alloy composites produced using friction stir processing. Trans Indian Inst Met 72:1593–1596
171. Patel V, Li W, Wang G, Wang F, Vairis A, Niu P (2019) Friction stir welding of dissimilar aluminum alloy combinations: state-of-the-art. Metals 9:270
172. Jacquin D, Guillemot G (2021) A review of microstructural changes occurring during FSW in aluminium alloys and their modelling. J Mater Process Technol 288:116706
173 Akinlabi ET, Mahamood R, Akinlabi SA, Ogunmuyiwa E (2014) Processing parameters influence on wear resistance behaviour of friction stir processed Al-TiC composites. Adv Mater Sci Eng 2014:724590
174. Zhang S, Chen G, Wei J, Liu Y, Xie R, Liu Q, Zeng S, Zhang G, Shi Q (2019) Effects of energy input during friction stir processing on microstructures and mechanical properties of aluminum/carbon nanotubes nanocomposites. J Alloy Compd 798:523–530
175. Sathish T, Kaladgi ARR, Mohanavel V, Arul K, Afzal A, Aabid A, Baig M, Saleh B (2021) Experimental investigation of the friction stir weldability of AA8006 with zirconia particle reinforcement and optimized process parameters. Materials 14:2782
176. Jain VKS, Varghese J, Muthukumaran S (2019) Effect of first and second passes on microstructure and wear properties of titanium dioxide-reinforced aluminum surface composite via friction stir processing. Arab J Sci Eng 44:949–957
177. Özcan ME (2022) The influence of parameters on the evolution of the friction surfacing method-a review. J Mech Sci Technol 36:723–730
178. Seidi E, Miller SF, Carlson BE (2021) Friction surfacing deposition by consumable tools. J Manuf Sci Eng 143:120801
179. Esther I, Dinaharan I, Murugan N (2019) Microstructure and wear characterization of AA2124/4wt.% B4C nano-composite coating on Ti− 6Al− 4V alloy using friction surfacing. Trans Nonferrous Met Soc China 29:1263–1274
180. Kallien Z, Rath L, Roos A, Klusemann B (2020) Experimentally established correlation of friction surfacing process temperature and deposit geometry. Surf Coat Technol 397:126040
181. Yu M, Zhao H, Zhang Z, Zhou L, Song X, Ma N (2021) Texture evolution and corrosion behavior of the AA6061 coating deposited by friction surfacing. J Mater Process Technol 291:117005
182. Silva K, Brito P, Santos I, Câmara M, Abrão A (2020) The behaviour of AISI 4340 steel coatings on low carbon steel substrate produced by friction surfacing. Surf Coat Technol 399:126170
183. Agiwal H, Sridharan K, Pfefferkorn FE, Yeom H (2022) Microstructure and corrosion behavior of friction-surfaced 304L austenitic stainless steels. Int J Adv Manuf Technol 122:1641–1649
184. Zhou L, Yu M, Liu B, Zhang Z, Liu S, Song X, Zhao H (2020) Microstructure and mechanical properties of Al/steel dissimilar welds fabricated by friction surfacing assisted friction stir lap welding. J Market Res 9:212–221
185. Pirhayati P, Aval HJ (2020) Microstructural characterization and mechanical properties of friction surfaced AA2024− Ag composites. Trans Nonferrous Met Soc China 30:1756–1770
186. Bararpour SM, Aval HJ, Jamaati R (2020) Effects of Zn powder on alloying during friction surfacing of Al–Mg alloy. J Alloy Compd 818:152823
187. Li H, Qin W, Galloway A, Toumpis A (2019) Friction surfacing of aluminium alloy 5083 on DH36 steel plate. Metals 9:479
188. Daniel SCJ, Damodaram R, Karthik G, Lakshmana Rao B (2022) Friction surfaced alloy 718 deposits: effect of process parameters on coating performance. J Mater Eng Perform 31:4119–4132. https://doi.org/10.1007/s11665-021-06488-4
189. Gopan V, Wins KLD, Surendran A (2021) Innovative potential of additive friction stir deposition among current laser based metal additive manufacturing processes: A review. CIRP J Manuf Sci Technol 32:228–248
190. Venkit H, Selvaraj SK (2022) Review on latest trends in friction-based additive manufacturing techniques. Proc Inst Mech Eng C J Mech Eng Sci 236:10090–10121

191. Li X, Li X, Hu S, Liu Y, Ma D (2024) Additive friction stir deposition: a review on processes, parameters, characteristics, and applications. Int J Adv Manuf Technol 133:1111–1128. https://doi.org/10.1007/s00170-024-13890-4
192. Agrawal P, Haridas RS, Yadav S, Thapliyal S, Gaddam S, Verma R, Mishra RS (2021) Processing-structure-property correlation in additive friction stir deposited Ti-6Al-4V alloy from recycled metal chips. Addit Manuf 47:102259
193. Anderson-Wedge K, Avery D, Daniewicz S, Sowards J, Allison P, Jordon J, Amaro R (2021) Characterization of the fatigue behavior of additive friction stir-deposition AA2219. Int J Fatigue 142:105951
194. Garcia D, Hartley WD, Rauch HA, Griffiths RJ, Wang R, Kong ZJ, Zhu Y, Hang ZY (2020) In situ investigation into temperature evolution and heat generation during additive friction stir deposition: A comparative study of Cu and Al-Mg-Si. Addit Manuf 34:101386
195. Phillips B, Avery D, Liu T, Rodriguez O, Mason C, Jordon J, Brewer L, Allison P (2019) Microstructure-deformation relationship of additive friction stir-deposition Al–Mg–Si. Materialia 7:100387
196. Rutherford BA, Avery DZ, Phillips BJ, Rao HM, Doherty KJ, Allison PG, Brewer LN, Jordon JB (2020) Effect of thermomechanical processing on fatigue behavior in solid-state additive manufacturing of Al-Mg-Si alloy. Metals 10:947
197. Derazkola HA, Simchi A (2020) Processing and characterizations of polycarbonate/alumina nanocomposites by additive powder fed friction stir processing. Thin-Walled Struct 157:107086
198. Mukhopadhyay A, Saha P (2020) Mechanical and microstructural characterization of aluminium powder deposit made by friction stir based additive manufacturing. J Mater Process Technol 281:116648
199. Jordon JB, Allison PG, Phillips BJ, Avery DZ, Kinser RP, Brewer LN, Cox C, Doherty K (2020) Direct recycling of machine chips through a novel solid-state additive manufacturing process. Mater Des 193:108850
200. Yu HZ, Mishra RS (2021) Additive friction stir deposition: a deformation processing route to metal additive manufacturing. Mater Res Lett 9:71–83
201. Sabbar HM, Leman Z, Shamsudin SB, Tahir SM, Aiza Jaafar CN, Hanim MAA, Ismsrrubie ZN, Al-Alimi S (2021) AA7075-ZrO2 nanocomposites produced by the consecutive solid-state process: A review of characterisation and potential applications. Metals 11:805
202. Hartley WD, Garcia D, Yoder JK, Poczatek E, Forsmark JH, Luckey SG, Dillard DA, Hang ZY (2021) Solid-state cladding on thin automotive sheet metals enabled by additive friction stir deposition. J Mater Process Technol 291:117045
203. Martin LP, Luccitti A, Walluk M (2022) Repair of aluminum 6061 plate by additive friction stir deposition. Int J Adv Manuf Technol 118:759–773. https://doi.org/10.1007/s00170-021-07953-z
204. Griffiths RJ, Petersen DT, Garcia D, Yu HZ (2019) Additive friction stir-enabled solid-state additive manufacturing for the repair of 7075 aluminum alloy. Appl Sci 9:3486
205. Khodabakhshi F, Gerlich AP (2018) Potentials and strategies of solid-state additive friction-stir manufacturing technology: A critical review. J Manuf Process 36:77–92. https://doi.org/10.1016/j.jmapro.2018.09.030
206. Padhy G, Wu C, Gao S (2015) Auxiliary energy assisted friction stir welding–status review. Sci Technol Weld Join 20:631–649
207. Mohan DG, Gopi S (2018) Induction assisted friction stir welding: a review. Aust J Mech Eng 18(1):119–123. https://doi.org/10.1080/14484846.2018.1432089
208. Campanelli SL, Casalino G, Casavola C, Moramarco V (2013) Analysis and comparison of friction stir welding and laser assisted friction stir welding of aluminum alloy. Materials 6:5923–5941
209. Sajed M, Guerrero JWG, Derazkola HA (2023) A Literature Survey on Electrical-Current-Assisted Friction Stir Welding. Appl Sci 13:1563. https://doi.org/10.3390/app13031563
210. Tripathi AM, Singh R, Chaudhary R, Kant R (2024) Hybrid energy assisted friction stir welding using secondary heating sources. Modern materials and manufacturing techniques. CRC Press, pp 120–153
211. Yaduwanshi DK, Bag S, Pal S (2014) Effect of Preheating in Hybrid Friction Stir Welding of Aluminum Alloy. J Mater Eng Perform 23:3794–3803. https://doi.org/10.1007/s11665-014-1170-x
212. Kumar S, Wu C, Padhy G, Ding W (2017) Application of ultrasonic vibrations in welding and metal processing: A status review. J Manuf Process 26:295–322
213. Selvaraj M, Murali V, Koteswara Rao S (2013) Mechanism of weld formation during friction stir welding of aluminum alloy. Mater Manuf Process 28:595–600
214. Saha R, Biswas P (2022) Thermomechanical analysis of induction assisted friction stir welding of Inconel 718 alloy: A finite element approach. Int J Press Vessels Pip 199:104731
215. Raj S, Biswas P (2022) High-frequency induction-assisted hybrid friction stir welding of Inconel 718 plates. J Manuf Sci Eng 144:041014
216. Raj S, Biswas P (2023) Effect of induction preheating on microstructure and mechanical properties of friction stir welded dissimilar material joints of Inconel 718 and SS316L. CIRP J Manuf Sci Technol 41:160–179
217. Ramon J, Pal M, Das B (2023) Investigation of Induction Heating Process for Selective Melting of Aluminum Alloy for the Repair of Exit Hole Defect in Friction Stir Welding Process. Arab J Sci Eng 48(9):12291–12311
218. Yang J, Oliveira J, Li Y, Tan C, Gao C, Zhao Y, Yu Z (2022) Laser techniques for dissimilar joining of aluminum alloys to steels: A critical review. J Mater Process Technol 301:117443
219. Shankar S, Mehta KP, Chattopadhyaya S, Vilaça P (2021) Chapter 9 - Hybrid welding technologies. In: Gupta K, Gupta K, Paulo Davim J (eds) Paulo Davim J. Advanced Welding and Deforming, Elsevier, pp 231–264
220. Wada T, Morisada Y, Sun Y, Fujii H, Kawahito Y, Matsushita M, Ikeda R (2020) Friction stir welding of medium carbon steel with laser-preheating. ISIJ Int 60:153–159
221. Ahmad B, Galloway A, Toumpis A (2019) Numerical optimisation of laser assisted friction stir welding of structural steel. Sci Technol Weld Joining 24:548–558
222. Li K, He X, Li L, Yang L, Hu J (2022) Residual stress distribution of aluminium-lithium alloy in hybrid process of friction stir welding and laser peening. Opt Laser Technol 152:108149
223. Bunaziv I, Akselsen OM, Ren X, Nyhus B, Eriksson M, Gulbrandsen-Dahl S (2021) A review on laser-assisted joining of aluminium alloys to other metals. Metals 11:1680
224. Sengupta K, Mondal AK, Bose D, Singh DK (2020) Fundamentals of electric resistance friction stir welding of metals: a review. In: IEEE 1st international conference for convergence in engineering (ICCE), Kolkata, India, pp 32–37. https://doi.org/10.1109/ICCE50343.2020.9290650
225. Han Y, Jiang X, Chen S, Yuan T, Zhang H, Bai Y, Xiang Y, Li X (2019) Microstructure and mechanical properties of electrically assisted friction stir welded AZ31B alloy joints. J Manuf Process 43:26–34. https://doi.org/10.1016/j.jmapro.2019.05.011

226. Luo J, Chen W, Fu G (2014) Hybrid-heat effects on electrical-current aided friction stir welding of steel, and Al and Mg alloys. J Mater Process Technol 214:3002–3012
227. Santos TG, Miranda R, Vilaça P (2014) Friction Stir Welding assisted by electrical Joule effect. J Mater Process Technol 214:2127–2133
228. Luo J, Wang X, Wang J (2009) New technological methods and designs of stir head in resistance friction stir welding. Sci Technol Weld Joining 14:650–654
229. Sengupta K, Chowdhury I, Banerjee A, Mondal AK, Bose D (2022) Analysis of suitability of WC tool for joining Inconel 601 alloy by electric assisted friction stir welding. Mater Today: Proc 60:2093–2098
230. Xiaoqing J, Yongyong L, Tao Y, Shujun C, Lei W, Wang J (2022) Enhanced mechanical properties of dissimilar Al and Mg alloys fabricated by pulse current assisted friction stir welding. J Manuf Process 76:123–137
231. Chen S, Wang L, Jiang X, Yuan T, Jiang W, Liu Y (2021) Microstructure and mechanical properties of AZ31B Mg alloy fabricated by friction stir welding with pulse current. J Manuf Process 71:317–328
232. Han Y, Chen S, Jiang X, Bai Y, Yuan T, Wang X (2021) Effect of microstructure, texture and deformation behavior on tensile properties of electrically assisted friction stir welded Ti-6Al-4 V joints. Mater Charact 176:111141
233. Chen S, Zhang H, Jiang X, Yuan T, Han Y, Li X (2019) Mechanical properties of electric assisted friction stir welded 2219 aluminum alloy. J Manuf Process 44:197–206
234. Kou S, Cao GP (2006) Arc-enhanced friction stir welding. US7078647
235. Bang H, Bang H, Jeon G, Oh I, Ro C (2012) Gas tungsten arc welding assisted hybrid friction stir welding of dissimilar materials Al6061-T6 aluminum alloy and STS304 stainless steel. Mater Des 37:48–55
236. Elanchezhian C, Ramnath BV, Pazhanivel K, Vedhapuri A, Mano B, Manojkumar A, Stalin M, Vishnu V (2015) Comparative study and analysis of friction stir welding with plasma arc welding. Appl Mech Mater 766:695–700
237. Li X, Chen S, Yuan T, Jiang X, Han Y (2020) Improving the properties of friction stir welded 2219–T87 aluminum alloy with GTA offset preheating. J Manuf Process 51:10–18
238. Yi T, Liu S, Fang C, Jiang G (2022) Eliminating hole defects and improving microstructure and mechanical properties of friction stir welded joint of 2519 aluminum alloy via TIG arc. J Mater Process Technol 310:117773
239. Pankaj P, Tiwari A, Biswas P, Rao AG (2021) Plasma-assisted hybrid dissimilar friction stir welding for joining of DH36 steel and AISI 1008 steel: thermal modelling and experimental analysis. Arab J Sci Eng 46:7929–7952
240. Kumar A, Pankaj P, Biswas P, Rao A (2022) Finite element analysis and experimental investigation on effect of process parameters in plasma-assisted friction stir welding of low carbon steel. Trans Indian Inst Met 75:2559–2579
241. Rusinko A (2011) Analytical description of ultrasonic hardening and softening. Ultrasonics 51:709–714. https://doi.org/10.1016/j.ultras.2011.02.003
242. Shi L, Wu CS, Sun Z (2017) An integrated model for analysing the effects of ultrasonic vibration on tool torque and thermal processes in friction stir welding. Sci Technol Weld Join 23:365–379. https://doi.org/10.1080/13621718.2017.1399545
243. Shi L, Wu C, Fu L (2020) Effects of tool shoulder size on the thermal process and material flow behaviors in ultrasonic vibration enhanced friction stir welding. J Manuf Process 53:69–83
244. Muhammad NA, Geng P, Wu C, Ma N (2023) Unravelling the ultrasonic effect on residual stress and microstructure in dissimilar ultrasonic-assisted friction stir welding of Al/Mg alloys. Int J Mach Tools Manuf 186:104004
245. Kumar S, Kumar D, Singh I, Rath D (2022) An insight into ultrasonic vibration assisted conventional manufacturing processes: A comprehensive review. Adv Mech Eng 14:16878132221107812
246. Lindamood LR, Matheny MP, Graff KF (2023) Chapter 10 - Ultrasonic welding of metals☆. In: Graff KF, Lucas M (eds) Gallego-Juárez JA. Woodhead Publishing, Power Ultrasonics (Second Edition), pp 163–204
247. Kumar S, Ding W, Sun Z, Wu C (2018) Analysis of the dynamic performance of a complex ultrasonic horn for application in friction stir welding. Int J Adv Manuf Technol 97:1269–1284
248. Kumar S (2016) Ultrasonic assisted friction stir processing of 6063 aluminum alloy. Arch Civil Mech Eng 16:473–484
249. Kumar S, Wu C (2020) Suppression of intermetallic reaction layer by ultrasonic assistance during friction stir welding of Al and Mg based alloys. J Alloys Comp 827:154343. https://doi.org/10.1016/j.jallcom.2020.154343
250. Kumar S, Wu C, Gao S (2020) Process parametric dependency of axial downward force and macro-and microstructural morphologies in ultrasonically assisted friction stir welding of Al/Mg alloys. Metall and Mater Trans A 51:2863–2881
251. Ruilin L, Diqiu H, Luocheng L, Shaoyong Y, Kunyu Y (2014) A study of the temperature field during ultrasonic-assisted friction-stir welding. Int J Adv Manuf Technol 73:321–327
252. Zhang Z, He C, Li Y, Yu L, Zhao S, Zhao X (2020) Effects of ultrasonic assisted friction stir welding on flow behavior, microstructure and mechanical properties of 7N01-T4 aluminum alloy joints. J Mater Sci Technol 43:1–13
253. Strass B, Wagner G, Eifler D (2014) Realization of Al/Mg-hybrid-joints by ultrasound supported friction stir welding. Trans Tech Publ, Materials Science Forum, pp 1814–1819
254. Thomä M, Wagner G, Straß B, Wolter B, Benfer S, Fürbeth W (2018) Ultrasound enhanced friction stir welding of aluminum and steel: Process and properties of EN AW 6061/DC04-Joints. J Mater Sci Technol 34:163–172
255. Liu X, Wu C, Padhy GK (2015) Improved weld macrosection, microstructure and mechanical properties of 2024Al-T4 butt joints in ultrasonic vibration enhanced friction stir welding. Sci Technol Weld Join 20:345–352
256. Liu X, Wu CS, Rethmeier M, Pittner A (2013) Mechanical properties of 2024–T4 aluminium alloy joints in ultrasonic vibration enhanced friction stir welding. China Weldng 22:8–13
257. Zhao J, Wu C, Su H (2021) Acoustic effect on the tensile properties and metallurgical structures of dissimilar friction stir welding joints of Al/Mg alloys. J Manuf Process 65:328–341
258. Shi L, Wu C, Liu X (2015) Modeling the effects of ultrasonic vibration on friction stir welding. J Mater Process Technol 222:91–102
259. Meng X, Jin Y, Ji S, Yan D (2018) Improving friction stir weldability of Al/Mg alloys via ultrasonically diminishing pin adhesion. J Mater Sci Technol 34:1817–1822
260. You J, Zhao Y, Dong C, Su Y (2023) Improving the microstructure and mechanical properties of Al-Cu dissimilar joints by ultrasonic dynamic-stationary shoulder friction stir welding. J Mater Process Technol 311:117812
261. Muhammad NA, Wu C (2019) Ultrasonic vibration assisted friction stir welding of aluminium alloy and pure copper. J Manuf Process 39:114–127
262. Zhao J, Wu C, Shi L (2022) Effect of ultrasonic field on microstructure evolution in friction stir welding of dissimilar Al/Mg alloys. J Market Res 17:1–21
263. Zhao J, Wu CS, Su H (2021) Ultrasonic effect on thickness variations of intermetallic compound layers in friction stir welding of aluminium/magnesium alloys. J Manuf Process 62:388–402

264. Zhao W, Wu C, Su H (2020) Numerical investigation of heat generation and plastic deformation in ultrasonic assisted friction stir welding. J Manuf Process 56:967–980
265. Zhao W, Wu C, Shi L (2021) Acoustic induced antifriction and its effect on thermo-mechanical behavior in ultrasonic assisted friction stir welding. Int J Mech Sci 190:106039